THE EUROPEAN
PHYSICAL JOURNAL C

CrossMark

Regular Article - Experimental Physics

Measurement of b hadron lifetimes in pp collisions at $\sqrt{s} = 8\,\text{TeV}$

CMS Collaboration*

CERN, 1211 Geneva 23, Switzerland

Abstract Measurements are presented of the lifetimes of the B^0, B_s^0, Λ_b^0, and B_c^+ hadrons using the decay channels $B^0 \rightarrow J/\psi K^*(892)^0$, $B^0 \rightarrow J/\psi K_S^0$, $B_s^0 \rightarrow J/\psi \pi^+\pi^-$, $B_s^0 \rightarrow J/\psi \phi(1020)$, $\Lambda_b^0 \rightarrow J/\psi \Lambda^0$, and $B_c^+ \rightarrow J/\psi \pi^+$. The data sample, corresponding to an integrated luminosity of $19.7\,\text{fb}^{-1}$, was collected by the CMS detector at the LHC in proton–proton collisions at $\sqrt{s} = 8\,\text{TeV}$. The B^0 lifetime is measured to be $453.0 \pm 1.6\,(\text{stat}) \pm 1.8\,(\text{syst})\,\mu\text{m}$ in $J/\psi K^*(892)^0$ and $457.8 \pm 2.7\,(\text{stat}) \pm 2.8\,(\text{syst})\,\mu\text{m}$ in $J/\psi K_S^0$, which results in a combined measurement of $c\tau_{B^0} = 454.1 \pm 1.4\,(\text{stat}) \pm 1.7\,(\text{syst})\,\mu\text{m}$. The effective lifetime of the B_s^0 meson is measured in two decay modes, with contributions from different amounts of the heavy and light eigenstates. This results in two different measured lifetimes: $c\tau_{B_s^0 \rightarrow J/\psi \pi^+\pi^-} = 502.7 \pm 10.2\,(\text{stat}) \pm 3.4\,(\text{syst})\,\mu\text{m}$ and $c\tau_{B_s^0 \rightarrow J/\psi \phi(1020)} = 443.9 \pm 2.0\,(\text{stat}) \pm 1.5\,(\text{syst})\,\mu\text{m}$. The Λ_b^0 lifetime is found to be $442.9 \pm 8.2\,(\text{stat}) \pm 2.8\,(\text{syst})\,\mu\text{m}$. The precision from each of these channels is as good as or better than previous measurements. The B_c^+ lifetime, measured with respect to the B^+ to reduce the systematic uncertainty, is $162.3 \pm 7.8\,(\text{stat}) \pm 4.2\,(\text{syst}) \pm 0.1\,(\tau_{B^+})\,\mu\text{m}$. All results are in agreement with current world-average values.

1 Introduction

Precise lifetime measurements involving the weak interaction play an important role in the study of nonperturbative aspects of quantum chromodynamics (QCD). The phenomenology is commonly described by the QCD-inspired heavy-quark expansion model, which provides estimates of the ratio of lifetimes for hadrons containing a common heavy quark [1]. In this paper, we report measurements of the lifetimes of the B^0, B_s^0, Λ_b^0, and B_c^+ hadrons.

The measurements are based on the reconstruction of the transverse decay length L_{xy}, where $\vec{L}_{xy}$ is defined as the flight distance vector from the primary vertex to the decay vertex of the b hadron, projected onto the transverse component $\vec{p}_T$

* e-mail: cms-publication-committee-chair@cern.ch

(perpendicular to the beam axis) of the b hadron momentum. The proper decay time of the b hadron times the speed of light is measured using

$$ct = cL_{xy}\frac{M}{p_T}, \qquad (1)$$

where M is the world-average value of the mass of the b hadron [2].

In this analysis, the b hadrons are reconstructed from decays containing a J/ψ meson. The data were recorded by the CMS detector [3] at the CERN LHC using dedicated triggers that require two oppositely charged muons consistent with originating from a common vertex and with an invariant mass compatible with that of the J/ψ meson. Specifically, we reconstruct the decay modes $B^0 \rightarrow J/\psi K^*(892)^0$, $B^0 \rightarrow J/\psi K_S^0$, $B_s^0 \rightarrow J/\psi \pi^+\pi^-$, $B_s^0 \rightarrow J/\psi \phi(1020)$, $\Lambda_b^0 \rightarrow J/\psi \Lambda^0$, and $B_c^+ \rightarrow J/\psi \pi^+$, where $J/\psi \rightarrow \mu^+\mu^-$, $K^*(892)^0 \rightarrow K^+\pi^-$, $K_S^0 \rightarrow \pi^+\pi^-$, $\phi(1020) \rightarrow K^+K^-$, and $\Lambda^0 \rightarrow p\pi^-$. The $B^+ \rightarrow J/\psi K^+$ decay is used as a reference mode and in evaluating some of the systematic uncertainties. Charge conjugation is implied throughout, unless otherwise indicated.

The decay rate of neutral B_q (q = s or d) mesons is characterized by two parameters: the average decay width $\Gamma_q = (\Gamma_L^q + \Gamma_H^q)/2$ and the decay width difference $\Delta\Gamma_q = \Gamma_L^q - \Gamma_H^q$, where $\Gamma_{L,H}^q$ are the decay widths of the light (L) and heavy (H) mass eigenstates. Assuming equal amounts of B_q and its antiparticle are produced in the proton–proton collisions, the time-dependent decay rate into a final state f that is accessible by both particle and antiparticle can be written as [4]:

$$R_L^f e^{-\Gamma_L^q t} + R_H^f e^{-\Gamma_H^q t}, \qquad (2)$$

where R_L^f and R_H^f are the amplitudes of the light and heavy mass states, respectively. Since the neutral B mesons have two eigenstates with different lifetimes, the ct distribution consists of the sum of two exponential contributions. The

effective lifetime of the neutral B_q meson, produced as an equal admixture of particle and antiparticle flavour eigenstates and decaying into a final state f, can be written as [4]:

$$\tau_{\text{eff}} = \frac{\frac{R_{\text{L}}^f}{(\Gamma_{\text{L}}^q)^2} + \frac{R_{\text{H}}^f}{(\Gamma_{\text{H}}^q)^2}}{\frac{R_{\text{L}}^f}{\Gamma_{\text{L}}^q} + \frac{R_{\text{H}}^f}{\Gamma_{\text{H}}^q}}. \tag{3}$$

Since the amplitudes R_{H}^f and R_{L}^f are specific to the decay channel, the effective lifetime depends on the final state f and is measured by fitting an exponential function to a distribution consisting of the sum of two exponential contributions. Because the B^0 system has a small lifetime difference with respect to the average lifetime, $\Delta\Gamma_{\text{d}}/\Gamma_{\text{d}} = (-0.2 \pm 1.0)\%$ [5], the ct distribution is close to an exponential, and it is treated as such for the lifetime measurement. Following Ref. [6], the B^0 lifetimes measured in the flavour-specific channel $B^0 \to J/\psi K^*(892)^0$ and the CP eigenstate channel $B^0 \to J/\psi K_{\text{S}}^0$ are used to determine values for $\Delta\Gamma_{\text{d}}$, Γ_{d}, and $\Delta\Gamma_{\text{d}}/\Gamma_{\text{d}}$.

In the B_s^0 system, $\Delta\Gamma_{\text{s}}/\Gamma_{\text{s}} = (13.0 \pm 0.9)\%$ [5] and the deviation from an exponential ct distribution is sizeable. In this analysis, the two lifetimes associated with the B_s^0 meson are measured in the $J/\psi\pi^+\pi^-$ and $J/\psi\phi(1020)$ decay channels. The $B_s^0 \to J/\psi\pi^+\pi^-$ decays are reconstructed in the invariant mass range $0.9240 < M(\pi^+\pi^-) < 1.0204\,\text{GeV}$, which is dominated by the $f_0(980)$ resonance [7,8], making it a CP-odd final state. Therefore, the lifetime measured in this channel is related to the inverse of the decay width of the heavy B_s^0 mass eigenstate, $\tau_{B_s^0}^{\text{CP-odd}} \approx 1/\Gamma_{\text{H}}$, as CP violation in mixing is measured to be negligible [2]. The $J/\psi\phi(1020)$ decay channel is an admixture of CP-even and CP-odd states, corresponding to the light and heavy mass eigenstates, respectively, neglecting CP violation in mixing. Rewriting Eq. (3), the effective lifetime of the B_s^0 meson decaying to $J/\psi\phi(1020)$ can be expressed as

$$\tau_{\text{eff}} = f_{\text{H}}\tau_{\text{H}} + (1 - f_{\text{H}})\tau_{\text{L}}, \tag{4}$$

where τ_{L} and τ_{H} are the lifetimes of the light and heavy mass states, respectively, and f_{H} is the heavy-component fraction, defined as:

$$f_{\text{H}} = \frac{|A_\perp|^2\tau_{\text{H}}}{|A|^2\tau_{\text{L}} + |A_\perp|^2\tau_{\text{H}}}. \tag{5}$$

Here, $|A|^2 = |A_0(0)|^2 + |A_\parallel(0)|^2$ is the sum of the squares of the amplitudes of the two CP-even states, and $|A_\perp|^2 = |A_\perp(0)|^2$ is the square of the amplitude of the CP-odd state. The amplitudes are determined at the production time $t = 0$. Normalization constraints require $|A|^2 = 1 - |A_\perp|^2$ and therefore

$$f_{\text{H}} = \frac{|A_\perp|^2\tau_{\text{H}}}{(1 - |A_\perp|^2)\tau_{\text{L}} + |A_\perp|^2\tau_{\text{H}}}. \tag{6}$$

By combining the B_s^0 lifetimes obtained from the final states $J/\psi\phi(1020)$ and $J/\psi\pi^+\pi^-$, it is possible to determine the lifetime of the light B_s^0 mass eigenstate. The results in this paper are complementary to the CMS weak mixing phase analysis in the $B_s^0 \to J/\psi\phi(1020)$ channel [9], which provided measurements of the average decay width Γ_{s} and the decay width difference $\Delta\Gamma_{\text{s}}$.

The weak decay of the B_c^+ meson can occur through either the b or c quark decaying, with the other quark as a spectator, or through an annihilation process. The latter is predicted to contribute 10% of the decay width [10], and lifetime measurements can be used to test the B_c^+ decay model. As fewer and less precise measurements of the B_c^+ lifetime exist [11–16] compared to other b hadrons, the B_c^+ lifetime measurement presented in this paper is particularly valuable.

2 The CMS detector

The central feature of the CMS apparatus is a superconducting solenoid of 6 m internal diameter, providing a magnetic field of 3.8 T. Within the solenoid volume are a silicon pixel and strip tracker, a lead tungstate crystal electromagnetic calorimeter, and a brass and scintillator hadron calorimeter, each composed of a barrel and two endcap sections. Forward calorimeters extend the pseudorapidity coverage provided by the barrel and endcap detectors. Muons are detected in gasionization chambers embedded in the steel flux-return yoke outside the solenoid.

The main subdetectors used for this analysis are the silicon tracker and the muon detection system. The silicon tracker measures charged particles in the pseudorapidity range $|\eta| < 2.5$. It consists of 1440 silicon pixel and 15 148 silicon strip detector modules. For charged particles of $1 < p_{\text{T}} < 10\,\text{GeV}$ and $|\eta| < 1.4$, the track resolutions are typically 1.5% in p_{T} and 25–90 (45–150) μm in the transverse (longitudinal) impact parameter [17]. Muons are measured in the pseudorapidity range $|\eta| < 2.4$, with detection planes made using three technologies: drift tubes, cathode strip chambers, and resistive-plate chambers.

Events of interest are selected using a two-tiered trigger system [18]. The first level, composed of custom hardware processors, uses information from the calorimeters and muon detectors to select events at a rate of around 100 kHz within a time interval of less than 4 μs. The second level, known as the high-level trigger (HLT), consists of a farm of processors running a version of the full event reconstruction software optimized for fast processing, and reduces the event rate to around 1 kHz before data storage. At the HLT stage, there is

full access to the event information, and therefore selection criteria similar to those applied offline can be used.

A more detailed description of the CMS detector, together with a definition of the coordinate system used and the relevant kinematic variables, can be found in Ref. [3].

3 Data and Monte Carlo simulated samples

The data used in this analysis were collected in 2012 from proton–proton collisions at a centre-of-mass energy of 8 TeV, and correspond to an integrated luminosity of 19.7 fb^{-1}.

Fully simulated Monte Carlo (MC) samples of $B^+ \rightarrow J/\psi K^+$, $B^0 \rightarrow J/\psi K^*(892)^0$, $B^0 \rightarrow J/\psi K_S^0$, $B_s^0 \rightarrow J/\psi \pi^+ \pi^-$, $B_s^0 \rightarrow J/\psi \phi(1020)$, and $\Lambda_b^0 \rightarrow J/\psi \Lambda^0$ were produced with PYTHIA 6.424 [19] to simulate the proton–proton collisions, and subsequent parton shower and hadronization processes. The B_c^+ MC sample was produced with the dedicated generator BCVEGPY 2.0 [20,21] interfaced to PYTHIA. Decays of particles containing b or c quarks are simulated with the EVTGEN package [22], and final-state radiation is included via PHOTOS [23]. Events are passed through the CMS detector simulation based on GEANT4 [24], including additional proton–proton collisions in the same or nearby beam crossings (pileup) to match the number of multiple vertices per event in the data. Simulated events are processed with the same reconstruction and trigger algorithms as the data.

4 Reconstruction of b hadrons

The data are collected with a trigger that is designed to identify events in which a J/ψ meson decays to two oppositely charged muons. The transverse momentum of the J/ψ candidate is required to be greater than 7.9 GeV and both muons must be in the pseudorapidity region $|\eta| < 2.2$. The distance of closest approach of each muon to the event vertex in the transverse plane must be less than 0.5 cm and a fit of the two muons to a common vertex must have a χ^2 probability greater than 0.5%. The invariant mass of the dimuon system must lie within ± 5 times the experimental mass resolution (typically about 35 MeV) of the world-average J/ψ mass [2].

The offline selection starts from J/ψ candidates that are reconstructed from pairs of oppositely charged muons. The standard CMS muon reconstruction procedure [25] is used to identify the muons, which requires multiple hits in the pixel, strip, and muon detectors with a consistent trajectory throughout. The offline selection requirements on the dimuon system replicate the trigger selection. From the sample of collected J/ψ events, candidate b hadrons are reconstructed by combining a J/ψ candidate with track(s) or reconstructed neutral particles, depending on the decay mode. Only tracks that pass the standard CMS high-purity requirements [17] are

used. The b hadron candidate is fitted to a common vertex with the appropriate masses assigned to the charged tracks and the dimuon invariant mass constrained to the world-average J/ψ mass [2]. In fits that include a K_S^0 or Λ^0 hadron, the world-average mass is used for those particles. Primary vertices (PV) are fitted from the reconstructed tracks using an estimate of the proton–proton interaction region (beamspot) as a constraint. The PV having the smallest pointing angle, defined as the angle between the reconstructed b hadron momentum and the vector joining the PV with the decay vertex, is used. As the proper decay times are measured in the transverse plane, where the PV position is dominated by the beamspot, the choice of PV has little effect on the analysis and is accounted for as a systematic uncertainty.

4.1 Reconstruction of B^+, B^0, B_s^0, and Λ_b^0 hadrons

The B^+, B^0, B_s^0, and Λ_b^0 hadrons are reconstructed in the decays $B^+ \rightarrow J/\psi K^+$, $B^0 \rightarrow J/\psi K_S^0$, $B^0 \rightarrow J/\psi K^*(892)^0$, $B_s^0 \rightarrow J/\psi \pi^+ \pi^-$, $B_s^0 \rightarrow J/\psi \phi(1020)$, and $\Lambda_b^0 \rightarrow J/\psi \Lambda^0$. The $K^*(892)^0$, K_S^0, $\phi(1020)$, and Λ^0 candidates are reconstructed from pairs of oppositely charged tracks that are consistent with originating from a common vertex. Because of the lack of charged particle identification, the labelling of tracks as pions, kaons, and protons simply means the mass that is assigned to the track. The mass assignments for the K_S^0 and $\phi(1020)$ decay products are unambiguous (either both pions or both kaons). For the kinematic region considered in this analysis, simulations show that the proton always corresponds to the track with the larger momentum (leading track) from the Λ^0 decay. The $K^*(892)^0$ candidates are constructed from a pair of tracks with kaon and pion mass assignments.

Since two $K^*(892)^0$ candidates can be formed with a single pair of tracks, we select the combination for which the mass of the $K^*(892)^0$ candidate is closest to the world-average value [2]. This selects the correct combination 88% of the time.

All tracks must have a transverse momentum greater than 0.5 GeV. The decay vertices of the K_S^0 and Λ^0 particles are required to have a transverse decay length larger than 15σ and their two decay products must each have a transverse impact parameter of at least 2σ, where the distances are with respect to the beamspot and σ is the calculated uncertainty in the relevant quantity. The intermediate candidate states $K^*(892)^0$, K_S^0, $\phi(1020)$, and Λ^0 are selected if they lie within the following mass regions that correspond to 1–2 times the experimental resolution or natural width around the nominal mass: $0.7960 < M(K^+\pi^-) < 0.9880$ GeV, $0.4876 < M(\pi^+\pi^-) < 0.5076$ GeV, $1.0095 < M(K^+K^-) < 1.0295$ GeV, and $1.1096 < M(p\pi^-) < 1.1216$ GeV. The accepted mass region of the $\pi^+\pi^-$ system in $B_s^0 \rightarrow J/\psi \pi^+\pi^-$ decay is $0.9240 < M(\pi^+\pi^-) < 1.0204$ GeV. The K_S^0 contamination in the Λ^0 sample is removed by dis-

carding candidates in which the leading particle in the Λ^0 decay is assigned the pion mass and the resulting $\pi^+\pi^-$ invariant mass is in the range $0.4876 < M(\pi^+\pi^-) < 0.5076$ GeV. Conversely, the Λ^0 contamination is removed from the K_S^0 sample by discarding candidates in the $p\pi^-$ mass region $1.1096 < M(p\pi^-) < 1.1216$ GeV, when the proton mass is assigned to the leading pion from the K_S^0 decay. The p_T of the K^+ candidate track from the B^+ decay must be larger than 1 GeV. The p_T of the $\pi^+\pi^-$ system in $B_s^0 \to J/\psi\pi^+\pi^-$ decays and the $K^*(892)^0$ candidates in $B^0 \to J/\psi K^*(892)^0$ decays must be greater than 3.5 GeV, with the leading (trailing) charged hadrons in these decays required to have a p_T greater than 2.5 (1.5) GeV. The p_T of the b hadrons must be at least 13 GeV, except for the $B_s^0 \to J/\psi\phi(1020)$ decay where no requirement is imposed. The p_T of the leading track from the K_S^0 and Λ^0 decays must be larger than 1.8 GeV. The minimum p_T for the kaons forming a $\phi(1020)$ candidate is 0.7 GeV.

The b hadron vertex χ^2 probability is required to be greater than 0.1% in the $B_s^0 \to J/\psi\phi(1020)$ channel only. The lifetime measurement is limited to events in which the b hadron ct is greater than 0.02 cm to avoid resolution and reconstruction effects present in the low-ct region. No attempt is made to select a single b hadron candidate in the relatively rare ($< 1\%$) events in which more than one b hadron candidate is found.

4.2 Reconstruction of $B_c^+ \to J/\psi\pi^+$

The B_c^+ lifetime is measured using the method developed by the LHCb Collaboration [12] in which the measured difference in total widths between the B_c^+ and B^+ mesons is used in combination with the precisely known B^+ lifetime to obtain the B_c^+ lifetime. This method does not require modelling the background ct distribution, avoiding a source of systematic uncertainty. The same reconstruction algorithm and selection criteria are used for both decays, $B_c^+ \to J/\psi\pi^+$ and $B^+ \to J/\psi K^+$. As a result, the dependence of the efficiencies on the proper decay time is similar.

The charged hadron tracks are required to have at least 2 pixel hits, at least 6 tracker hits (strips and pixels together), a track fit χ^2 less than 3 times the number of degrees of freedom, and $|\eta| < 2.4$. The dimuon invariant mass is required to lie in the range $\pm 3\sigma$ from the nominal J/ψ meson mass, where σ is the average resolution for the J/ψ signal, which depends on the J/ψ pseudorapidity and ranges from 35 to 50 MeV. The p_T of the charged hadron tracks and the b hadrons are required to be greater than 3.3 and 10 GeV, respectively. The b hadrons must have a rapidity of $|y| < 2.2$, a vertex χ^2 probability greater than 5%, a dimuon vertex χ^2 probability greater than 1%, and $\cos\theta > 0.98$, where $\cos\theta = \vec{L}_{xy} \cdot \vec{p}_{T,B} / (|L_{xy}| \cdot |p_{T,B}|)$ and $\vec{L}_{xy}$ and $\vec{p}_{T,B}$ refer to the transverse decay length and momentum of the B^+ or

B_c^+ mesons. The lifetime measurement is limited to events in which the b hadron has $ct > 0.01$ cm, which ensures that the ratio of the B_c^+ to B^+ meson efficiencies is constant versus ct. The analysis of the B_c^+ lifetime is described in Sect. 6.

5 Measurement of the B^0, B_s^0, and Λ_b^0 lifetimes

For each decay channel, we perform a simultaneous fit to three input variables, the b hadron mass, ct, and ct uncertainty (σ_{ct}). For the B^+, B^0, and Λ_b^0 hadrons, an unbinned maximum-likelihood fit is performed with a probability density function (PDF) given by:

$$\text{PDF} = f_s\, M_s(M)\, T_s(ct)\, E_s(\sigma_{ct})\, \varepsilon(ct)$$
$$+ (1 - f_s)\, M_b(M)\, T_b(ct)\, E_b(\sigma_{ct}), \tag{7}$$

where f_s is the fraction of signal events, and M_s (M_b), T_s (T_b), and E_s (E_b) are the functions describing the signal (background) distributions of the b hadron mass, ct, and σ_{ct}, respectively, while ε is the efficiency function. These functions are derived below. For the B_s^0 modes, we use an extended maximum-likelihood fit in order to correctly incorporate background sources whose yields are obtained from the fit.
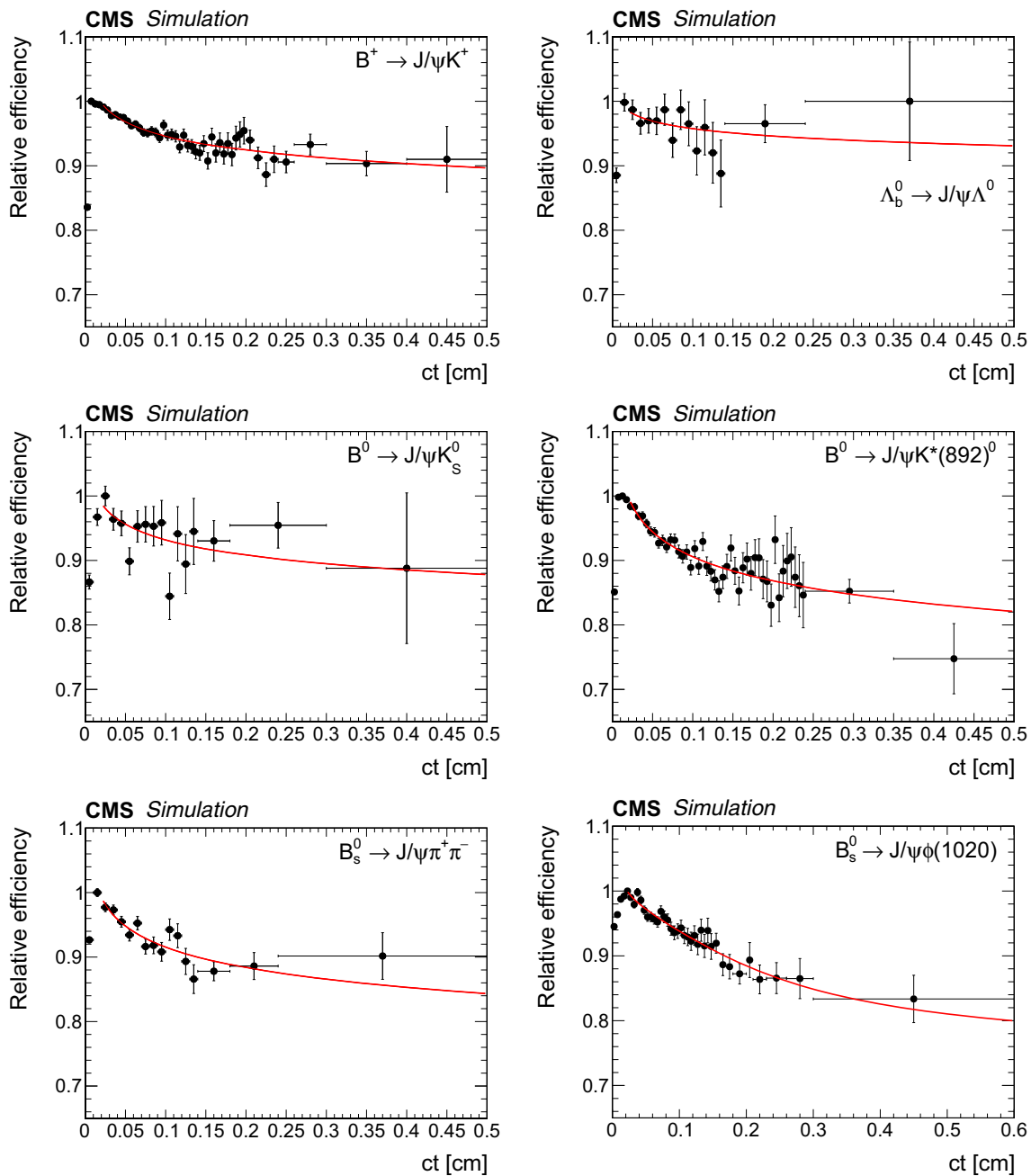
5.1 Reconstruction and selection efficiency

The reconstruction and selection efficiency ε for each decay mode is determined as a function of ct by using fully simulated MC samples. This efficiency is defined as the generated ct distribution of the selected events after reconstruction and selection divided by the ct distribution obtained from an exponential decay with the lifetime set to the value used to generate the events. The efficiency for the $B_s^0 \to J/\psi\phi(1020)$ channel is defined as the generated ct distribution of the selected events after reconstruction divided by the sum of the two exponentials generated with the theoretical $B_s^0 \to J/\psi\phi(1020)$ decay rate model [26]. In the theoretical model, the values of the physics parameters are set to those used in the simulated sample.

Figure 1 shows the efficiency as a function of ct for the various decay modes, with an arbitrary normalization since only the relative efficiency is relevant. The efficiencies display a sharp rise as ct increases from 0 to 0.01 cm, followed by a slow decrease as ct increases further. The ct efficiency is modelled with an inverse power function.

5.2 Data modelling

Depending on the decay channel, the invariant mass distribution for the signal M_s is modelled with one or two Gaussian functions, and a linear polynomial or an exponential

Fig. 1 The combined reconstruction and selection efficiency from simulation versus ct with a superimposed fit to an inverse power function for $B^+ \to J/\psi K^+$ (upper left), $\Lambda_b^0 \to J/\psi \Lambda^0$ (upper right), $B^0 \to J/\psi K_S^0$ (centre left), $B^0 \to J/\psi K^*(892)^0$ (centre right), $B_s^0 \to J/\psi \pi^+\pi^-$ (lower left), and $B_s^0 \to J/\psi \phi(1020)$ (lower right). The efficiency scale is arbitrary

function is used to model the combinatorial background M_b. For the $B_s^0 \to J/\psi \pi^+\pi^-$ decay, three additional terms are added to M_b to include specific sources of background. The $B^0 \to J/\psi \pi^+\pi^-$ decays are modelled by a Gaussian function, the $B^+ \to J/\psi K^+$ decays by a shape taken from simulation, and the $B^0_{(d,s)} \to J/\psi h_1^+ h_2^-$ decays, where h_1^+ and h_2^- are charged hadron tracks that are not both pions, by a Gaussian function.

The signal ct distribution T_s is modelled by an exponential function convolved with the detector resolution and then multiplied by the function describing the reconstruction and selection efficiency. The resolution is described by a Gaussian function with the per-event width taken from the ct uncertainty distribution. The backgrounds T_b are described by a superposition of exponential functions convolved with the resolution. The number of exponentials
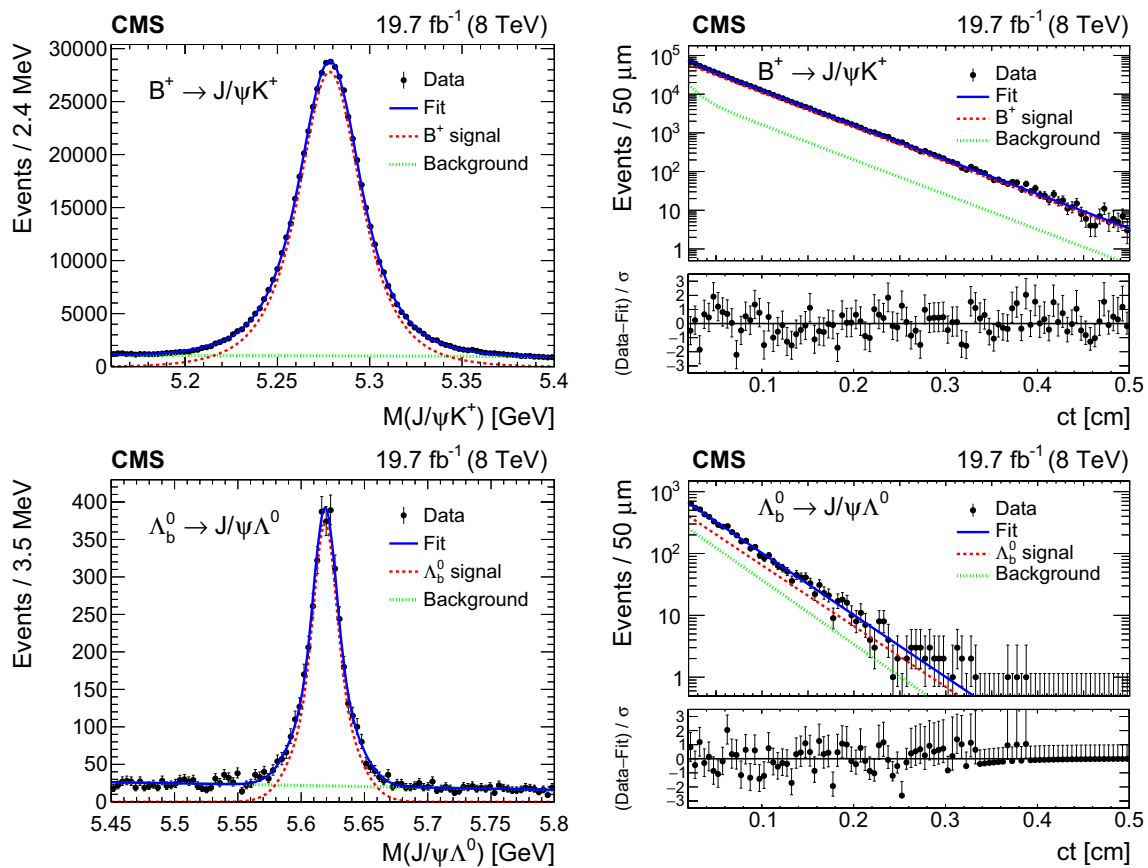
Fig. 2 Invariant mass (left) and ct (right) distributions for B^+ (upper) and for Λ_b^0 (lower) candidates. The curves are projections of the fit to the data, with the contributions from signal (dashed), background (dotted), and the sum of signal and background (solid) shown. the lower panels

of the figures on the right show the difference between the observed data and the fit divided by the data uncertainty. The vertical bars on the data points represent the statistical uncertainties

needed to describe the background is determined from data events in the mass sideband regions for each decay mode.

The signal E_s and background E_b σ_{ct} distributions are modelled with a sum of two gamma functions for the $B_s^0 \to J/\psi\phi(1020)$ channel and two exponential functions convolved with a Gaussian function for the other channels. The background parameters are obtained from a fit to the mass sideband distributions. The signal parameters are obtained from a fit to the signal region after subtracting the background contribution using the mass sideband region to estimate the background. The parameters of the efficiency function and the functions modelling the σ_{ct} distributions are kept constant in the fit. The remaining fit parameters are allowed to vary freely.

For the $B_s^0 \to J/\psi\pi^+\pi^-$ mode, the parameters of the mass model for the $B^+ \to J/\psi K^+$ contamination are taken from the simulation, and the yield and lifetime are determined by the fit. The mass of the $B^0 \to J/\psi\pi^+\pi^-$ contamination is fixed to the weighted average of the masses measured from our two B^0 decay modes, and the width of the Gaussian func-

tion is the same as the width used for the $B_s^0 \to J/\psi\pi^+\pi^-$ signal, corrected by a factor of $M_{B^0}/M_{B_s^0}$. The lifetime of this contamination is fixed to the world-average value, corrected by the same factor as the width, and the yield is a free parameter of the fit.

5.3 Fit results

The invariant mass and ct distributions obtained from data are shown with the fit results superimposed in Figs. 2, 3 and 4. The ct distributions are fitted in the range 0.02–0.50 cm for all modes except the $B_s^0 \to J/\psi\phi(1020)$ channel, where the upper limit is increased to 0.60 cm. The average lifetimes times the speed of light obtained from the fits are: $c\tau_{B^+} = 490.9 \pm 0.8\,\mu\text{m}$, $c\tau_{B^0 \to J/\psi K^*(892)^0} = 453.0 \pm 1.6\,\mu\text{m}$, $c\tau_{B^0 \to J/\psi K_S^0} = 457.8 \pm 2.7\,\mu\text{m}$, $c\tau_{B_s^0 \to J/\psi\pi^+\pi^-} = 502.7 \pm 10.2\,\mu\text{m}$, $c\tau_{B_s^0 \to J/\psi\phi(1020)} = 445.2 \pm 2.0\,\mu\text{m}$, and $c\tau_{\Lambda_b^0} = 442.9 \pm 8.2\,\mu\text{m}$, where all uncertainties are statistical only. The $B_s^0 \to J/\psi\phi(1020)$ value given here is uncorrected for two offsets described in Sect. 7. There is good agreement
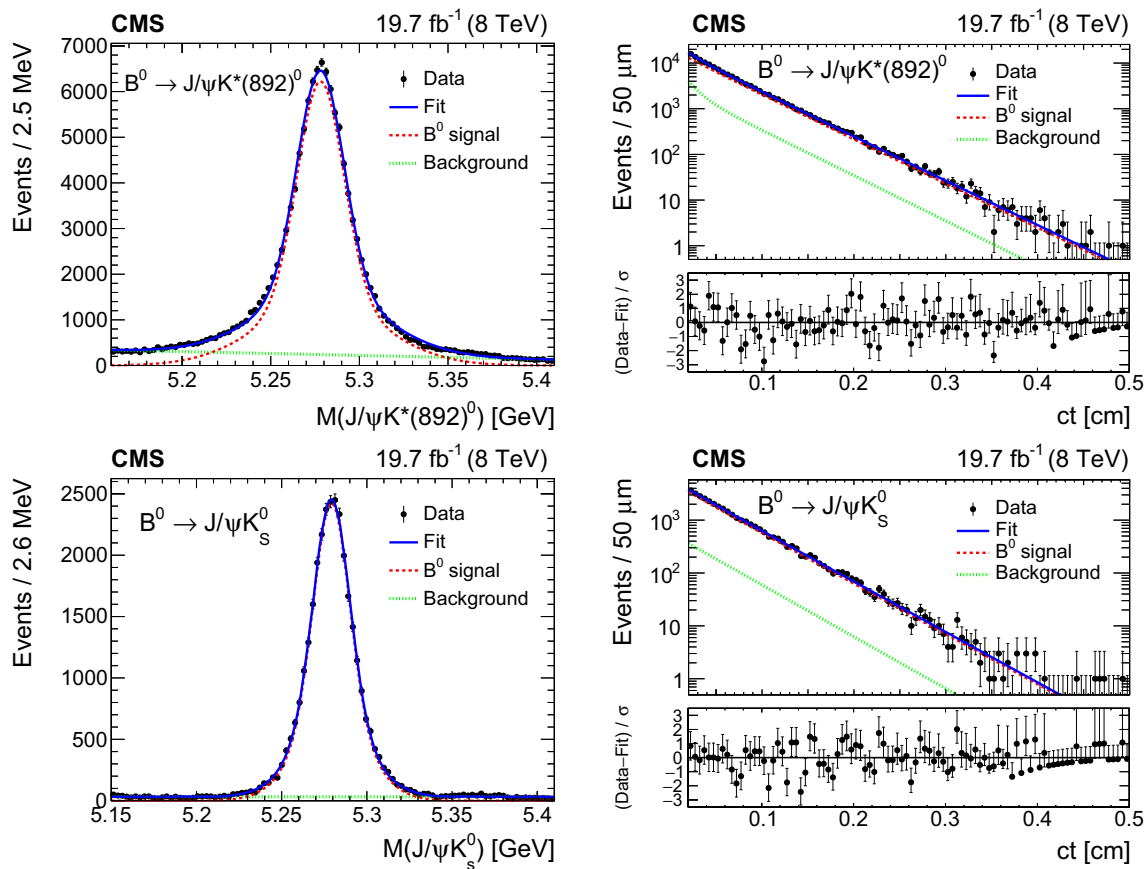
Fig. 3 Invariant mass (left) and ct (right) distributions for B^0 candidates reconstructed from $J/\psi K^*(892)^0$ (upper) and $J/\psi K^0_S$ (lower) decays. The curves are projections of the fit to the data, with the contributions from signal (dashed), background (dotted), and the sum of signal and background (solid) shown. the lower panels of the figures on the right show the difference between the observed data and the fit divided by the data uncertainty. The vertical bars on the data points represent the statistical uncertainties

between the fitted functions and the data. The probabilities calculated from the χ^2 of the ct distributions in Figs. 2, 3 and 4 all exceed 25%.

6 Measurement of the B^+_c lifetime

The decay time distribution for the signal $N_B(ct)$ can be expressed as the product of an efficiency function $\varepsilon_B(ct)$ and an exponential decay function $E_B(ct) = \exp(-ct/c\tau_B)$, convolved with the time resolution function of the detector $r(ct)$. The ratio of B^+_c to B^+ events at a given proper time can be expressed as

$$\frac{N_{B^+_c}(ct)}{N_{B^+}(ct)} \equiv R(ct) = \frac{\varepsilon_{B^+_c}(ct)[r(ct) \otimes E_{B^+_c}(ct)]}{\varepsilon_{B^+}(ct)[r(ct) \otimes E_{B^+}(ct)]}. \tag{8}$$

We have verified through studies of simulated pseudo-events that Eq. (8) is not significantly affected by the time resolution, and therefore this equation can be simplified to

$$R(ct) \approx R_\varepsilon(ct) \exp(-\Delta\Gamma t), \tag{9}$$

where the small effect from the time resolution is evaluated from MC simulations and is included in $R_\varepsilon(ct)$, which denotes the ratio of the B^+_c and B^+ efficiency functions. The quantity $\Delta\Gamma$ is defined as

$$\Delta\Gamma \equiv \Gamma_{B^+_c} - \Gamma_{B^+} = \frac{1}{\tau_{B^+_c}} - \frac{1}{\tau_{B^+}}. \tag{10}$$

The $B^+_c \to J/\psi\pi^+$ and $B^+ \to J/\psi K^+$ invariant mass distributions, shown in Fig. 5, are each fit with an unbinned maximum-likelihood estimator. The $J/\psi\pi^+$ invariant mass distribution is fitted with a Gaussian function for the B^+_c signal and an exponential function for the background. An additional background contribution from $B^+_c \to J/\psi K^+$ decays is modelled from a simulated sample of $B^+_c \to J/\psi K^+$ events, and its contribution is constrained using the value of the branching fraction relative to $J/\psi\pi^+$ [27]. The $B^+_c \to J/\psi\pi^+$ signal yield is 1128 ± 60 events, where the uncertainty is sta-
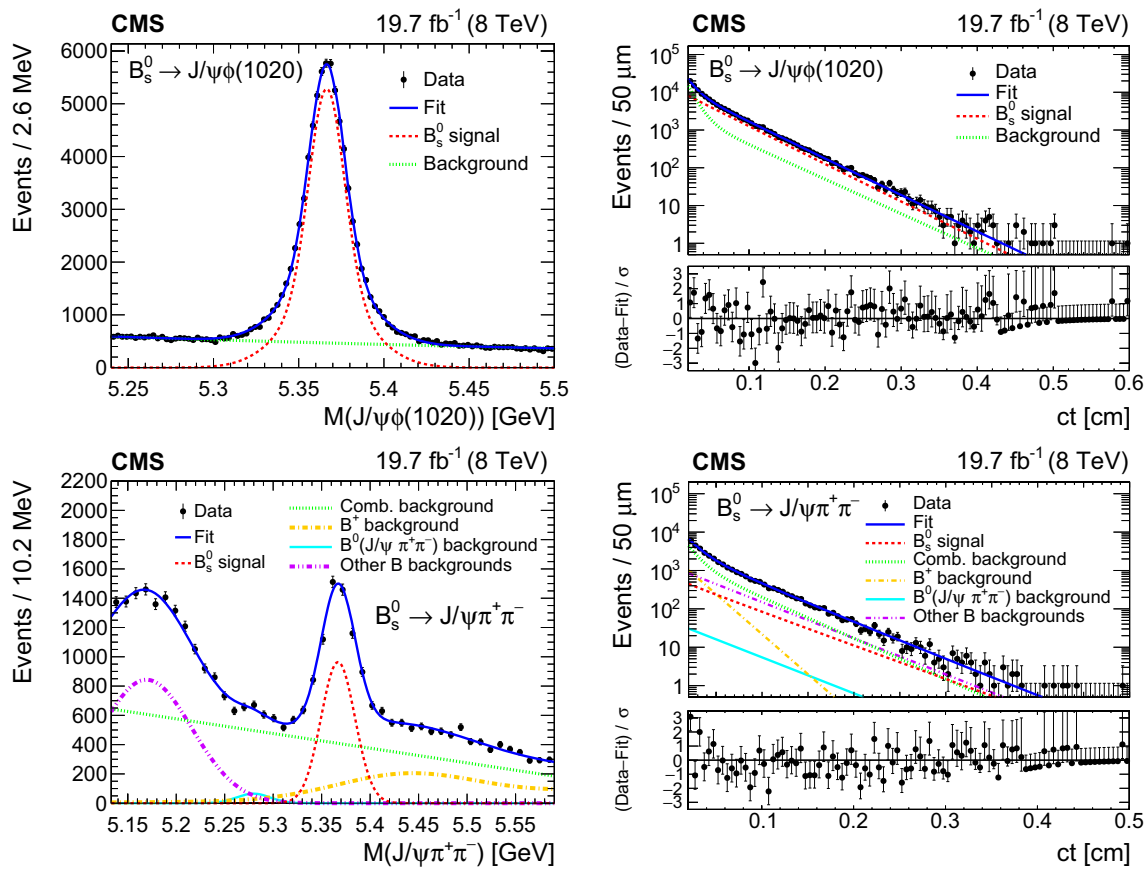
Fig. 4 Invariant mass (left) and ct (right) distributions for B_s^0 candidates reconstructed from $J/\psi\phi(1020)$ (upper) and $J/\psi\pi^+\pi^-$ (lower) decays. The curves are projections of the fit to the data, with the full fit function (solid) and signal (dashed) shown for both decays, the total background (dotted) shown for the upper plots, and the combinatorial background (dotted), misidentified $B^+ \to J/\psi K^+$ background (dashed-dotted), $B^0 \to J/\psi\pi^+\pi^-$ contribution (dashed-dotted-dotted-dotted), and partially reconstructed and other misidentified B backgrounds (dashed-dotted-dotted) shown for the lower plots. the lower panels of the figures on the right show the difference between the observed data and the fit divided by the data uncertainty. The vertical bars on the data points represent the statistical uncertainties

tistical only. The B^+ meson invariant mass distribution is fit with a sum of two Gaussian functions with a common mean for the signal and a second-order Chebyshev polynomial for the background. Additional contributions from partially reconstructed B^0 and B^+ meson decays are parametrized with functions determined from $B^+ \to J/\psi\pi^+$ and inclusive $B^0 \to J/\psi X$ MC samples.

6.1 The fit model and results

The B_c^+ lifetime is extracted through a binned χ^2 fit to the ratio of the efficiency-corrected ct distributions of the $B_c^+ \to J/\psi\pi^+$ and $B^+ \to J/\psi K^+$ channels. The B_c^+ and B^+ ct signal distributions from data are obtained by dividing the data sample into ct bins and performing an unbinned maximum-likelihood fit to the $J/\psi\pi^+$ and $J/\psi K^+$ invariant mass distribution in each bin, in the same manner as the fit to the full samples, except that the peak position and resolution are fixed to the values obtained by the fits to the full

samples. Varied ct bin widths are used to ensure a similar statistical uncertainty in the B_c^+ signal yield among the bins. The bin edges are defined by requiring a relative statistical uncertainty of 12% or better in each bin. The same binning is used for the B^+ ct distribution. The B_c^+ and B^+ meson yields are shown versus ct in the left plot of Fig. 6, where the number of signal events is normalized by the bin width. Efficiencies are obtained from the MC samples and are defined as the ct distribution of the selected events after reconstruction divided by the ct distribution obtained from an exponential decay with the lifetime set to the same value used to generate each MC sample. The ratio of the two efficiency distributions, using the same binning scheme as for the data, is shown in the right plot of Fig. 6.

The ratio of the B_c^+ to B^+ efficiency-corrected ct distributions, R/R_ε, is shown in Fig. 7, along with the result of a fit to an exponential function. The fit returns $\Delta\Gamma = 1.24 \pm 0.09$ ps^{-1}. Using the known lifetime of the B^+ meson, $c\tau_{B^+} = 491.1 \pm 1.2$ μm [5], a measurement of the B_c^+ meson life-
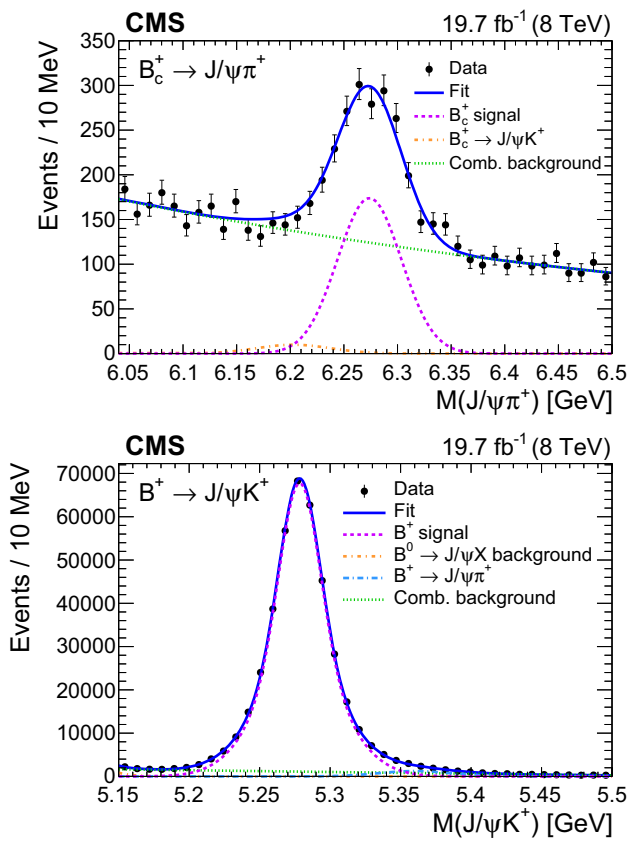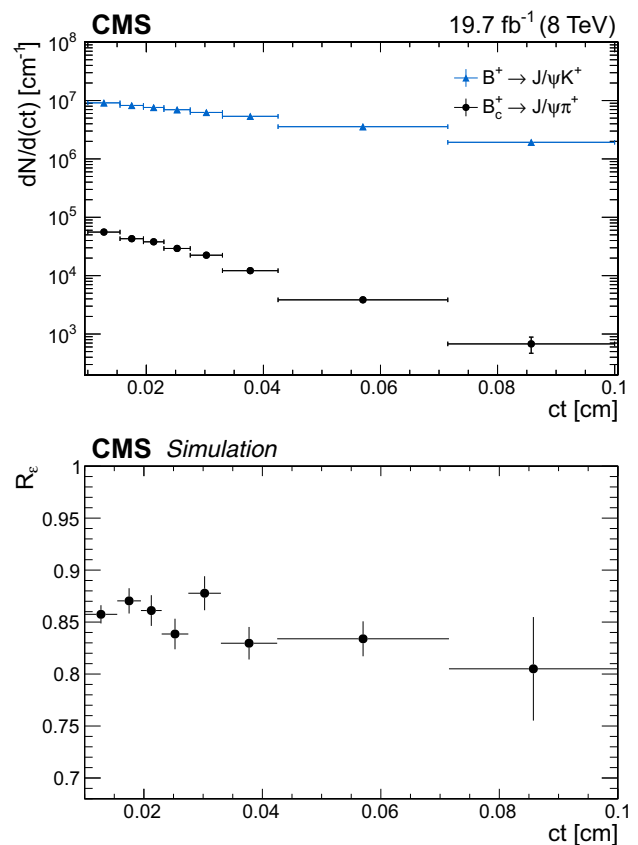
Fig. 5 The $J/\psi\pi^+$ invariant mass distribution (left) with the solid line representing the total fit, the dashed line the signal component, the dotted line the combinatorial background, and the dashed-dotted line the contribution from $B_c^+ \to J/\psi K^+$ decays. The $J/\psi K^+$ invariant mass distribution (right) with the solid line representing the total fit, the dashed line the signal component, the dotted-dashed curves the $B^+ \to J/\psi\pi^+$ and B^0 contributions, and the dotted curve the combinatorial background. The vertical bars on the data points represent the statistical uncertainties

Fig. 6 Yields of $B_c^+ \to J/\psi\pi^+$ and $B^+ \to J/\psi K^+$ events (left) as a function of ct, normalized to the bin width, as determined from fits to the invariant mass distributions. Ratio of the B_c^+ and B^+ efficiency distributions (right) as a function of ct, as determined from simulated events. The vertical bars on the data points represent the statistical uncertainties, and the horizontal bars show the bin widths

time, $c\tau_{B_c^+} = 162.3 \pm 7.8$ µm, is extracted, where the uncertainty is statistical only.

7 Systematic uncertainties

The systematic uncertainties can be divided into uncertainties common to all the measurements, and uncertainties specific to a decay channel. Table 1 summarizes the systematic uncertainties for the sources considered below and the total systematic uncertainty in the B_s^0, B^0, and Λ_b^0 lifetime measurements. The systematic uncertainties in $\Delta\Gamma$ and the B_c^+ meson lifetime are collected in Table 2. Using the known lifetime of the B^+ meson, the uncertainties in $\Delta\Gamma$ are converted into uncertainties in the B_c^+ meson lifetime measurement. The uncertainty in the B_c^+ meson lifetime due to the uncertainty in the B^+ meson lifetime [5] is quoted separately.

Fig. 7 Ratio of the B_c^+ to B^+ efficiency-corrected ct distributions, R/R_ε, with a line showing the result of the fit to an exponential function. The vertical bars give the statistical uncertainty in the data, and the horizontal bars show the bin widths

We have verified that the results are stable against changes in the selection requirements on the quality of the tracks and vertices, the kinematic variables, and ct, as well as in detector

Table 1 Summary of the sources and values of systematic uncertainties in the lifetime measurements (in μm). The total systematic uncertainty is the sum in quadrature of the individual uncertainties

Source	$B^0 \to J/\psi K^*(892)^0$	$B^0 \to J/\psi K_S^0$	$B_s^0 \to J/\psi \pi^+\pi^-$	$B_s^0 \to J/\psi \phi$	$\Lambda_b^0 \to J/\psi \Lambda^0$
MC statistical uncertainty	1.1	2.4	2.0	0.6	2.3
Mass modelling	0.3	0.4	0.2	0.4	0.9
ct modelling	0.1	0.1	0.4	0.0	0.1
B^+ contamination	–	–	1.4	–	–
Mass window of $\pi^+\pi^-$	–	–	1.8	–	–
$K^\pm\pi^\mp$ mass assignment	0.3	–	–	–	–
ct range	–	–	–	0.1	–
S-wave contamination	–	–	–	0.4	–
Absolute ct accuracy	1.3	1.3	1.4	1.3	1.3
Total (μm)	1.8	2.8	3.4	1.5	2.8

Table 2 Summary of the systematic uncertainties in the $\Delta\Gamma$ and $c\tau_{B_c^+}$ measurements

Source	$\Delta\Gamma$ (ps^{-1})	$c\tau_{B_c^+}$ (μm)
MC statistical uncertainty	0.01	1.2
Mass modelling	0.04	3.4
PV selection	0.02	2.0
Detector alignment	0.01	0.6
Total uncertainty	0.05	4.2

regions and data-taking periods. The effect of replacing the mass of the b hadron in the ct definition of Eq. (1) from the world-average to the reconstructed candidate mass is found to be negligible. The lifetimes for all decay channels were measured by treating MC samples as data. No bias was found and all results were consistent with the input lifetimes of the generated samples.

7.1 Common systematic uncertainties

1. Statistical uncertainty in the MC samples
   The number of events in the simulation directly affects the accuracy of the efficiency determination. In the case of the B_s^0, B^0, and Λ_b^0 lifetime measurements, 1000 efficiency curves are generated with variations of the parameter values. The parameter values are sampled using a multivariate Gaussian PDF that is constructed from the covariance matrix of the efficiency fit. The analysis is performed 1000 times, varying the parameters of the efficiency function. The distribution of the measured lifetimes is fitted with a Gaussian function, whose width is taken as the systematic uncertainty associated with the finite size of the simulated samples. In the measurement of the B_c^+ lifetime, the bin-by-bin statistical uncertainty in the efficiency determination is propagated to the $R(ct)$ distribution, the fit is performed, and the difference in

quadrature of the uncertainty in $\Delta\Gamma$ with respect to the nominal value is taken as the systematic uncertainty.

2. Modelling of the mass distribution shape
   Biases related to the modelling of the shapes of the b hadron mass signal and background PDFs are quantified by changing the signal and background PDFs individually and using the new models to fit the data. For the B^0, B_s^0, and Λ_b^0 lifetime measurements, the background model is changed to a higher-degree polynomial, a Chebyshev polynomial, or an exponential function, and the signal model is changed from two Gaussian functions to a single Gaussian function or a sum of three Gaussian functions. Differences in the measured lifetime between the results of the nominal and alternative models are used to estimate the systematic uncertainty, with the variations due to the modelling of signal and background components evaluated separately and added in quadrature. For the B_c^+ lifetime measurement, the signal peak is alternatively modelled with a Crystal Ball distribution [28]. The alternative description for the background is a first-order Chebyshev distribution. The removal of the Cabibbo-suppressed $B_c^+ \to J/\psi K^+$ contribution is also considered. The maximum deviation of the signal yield in each ct bin from the nominal value is propagated to the statistical uncertainty in the per-bin yield. The fit to $R(ct)$ is performed and the difference in quadrature between the uncertainty from this fit and the nominal measurement is taken as the systematic uncertainty.

7.2 Channel-specific systematic uncertainties

1. Modelling of the background ct shape in the B_s^0, B^0, and Λ_b^0 channels
   To estimate a systematic uncertainty due to the ct background model, we add an additional background contribution modelled with its own lifetime, and compare the result to that obtained with the nominal fit model. The

difference between the results of the nominal and alternative fit models is used as the systematic uncertainty from the ct shape modelling.

2. The B^+ contamination in the $B_s^0 \to J/\psi \pi^+ \pi^-$ sample
   In the nominal fit, the yield and lifetime of the $B^+ \to J/\psi K^+$ contamination are determined from the fit with the mass shape obtained from simulation. An alternative estimate of the $J/\psi K^+$ contamination is obtained from data by taking the leading pion of the $B_s^0 \to J/\psi \pi^+ \pi^-$ decay to be the kaon. The lifetime and yield of the $B^+ \to J/\psi K^+$ decays contaminating the $B_s^0 \to J/\psi \pi^+ \pi^-$ sample are determined from a fit of the B^+ signal candidates in the $B_s^0 \to J/\psi \pi^+ \pi^-$ sample, with the mass shape also obtained from the data. The difference between the B_s^0 lifetime found with this model and the nominal model is considered as the systematic uncertainty due to B^+ contamination.

3. Invariant mass window of the $\pi^+ \pi^-$ in the $B_s^0 \to J/\psi \pi^+ \pi^-$ channel
   Although the events selected by the $\pi^+ \pi^-$ mass window are dominated by the $f_0(980)$, its width is not well known and possible backgrounds under the $f_0(980)$ peak could be increased or decreased, depending on the mass window. The effect on the lifetime is studied by using mass windows of ± 30 and ± 80 MeV around the signal peak, compared to the nominal fit result with a ± 50 MeV window. The maximum variation of the lifetime is taken as the systematic uncertainty.

4. The $K^+ \pi^-$ mass assignments for $K^*(892)^0$ candidates in the $B^0 \to J/\psi K^*(892)^0$ channel
   The $K^*(892)^0$ candidates are constructed from a pair of tracks with kaon and pion mass assignments. The combination with invariant mass closest to the world-average $K^*(892)^0$ mass is chosen to reconstruct the B^0 candidate. To estimate the effect on the lifetime due to a possible misassignment of kaon and pion, both combinations are discarded if both are within the natural width of the $K^*(892)^0$ mass, and the difference between the lifetime obtained with this sample and the nominal sample is taken as the systematic uncertainty.

5. The ct range in the $B_s^0 \to J/\psi \phi(1020)$ channel
   Since the $ct > 0.02$ cm requirement distorts the fractions of heavy and light mass eigenstates, the measured B_s^0 effective lifetime must be corrected. The correction and systematic uncertainty are quantified analytically. The correction to the effective lifetime is

$$
\begin{aligned}
\delta_{ct} &= c\tau_{\text{eff}}^{\text{cut}} - c\tau_{\text{eff}} \\
&= \frac{(1 - |A_\perp|^2)(c\tau_L)^2 e^{-a/c\tau_L} + |A_\perp|^2 (c\tau_H)^2 e^{-a/c\tau_H}}{(1 - |A_\perp|^2)c\tau_L e^{-a/c\tau_L} + |A_\perp|^2 c\tau_H e^{-a/c\tau_H}} \\
&\quad - \frac{(1 - |A_\perp|^2)(c\tau_L)^2 + |A_\perp|^2 (c\tau_H)^2}{(1 - |A_\perp|^2)c\tau_L + |A_\perp|^2 c\tau_H},
\end{aligned}
\tag{11}
$$

where the first term represents the effective lifetime in the presence of a $ct > a$ requirement and the latter term is the unbiased effective lifetime. In this analysis, a is equal to 0.02 cm. The world-average values [2] for $c\tau_H = 482.7 \pm 3.6\,\mu$m, $c\tau_L = 426.3 \pm 2.4\,\mu$m, and $|A_\perp|^2 = 0.250 \pm 0.006$ are used to obtain the correction $\delta_{ct} = 0.62 \pm 0.10\,\mu$m.

6. The S-wave contamination in the $B_s^0 \to J/\psi \phi(1020)$ channel
   The B_s^0 candidates reconstructed in the $J/\psi \phi(1020)$ final state contain a small fraction of nonresonant and CP-odd $B_s^0 \to J/\psi K^+ K^-$ decays, where the invariant mass of the two kaons happens to be near the ϕ meson mass. The fraction of $B_s^0 \to J/\psi K^+ K^-$ decays among the selected events is measured in the weak mixing phase analysis [9] to be $f_S = (1.2^{+0.9}_{-0.7})\%$. Because of the different trigger and signal selection criteria of the present analysis, the S-wave fraction is corrected according to the simulation to be $(1.5^{+1.1}_{-0.9})\%$. The bias caused by the contamination of nonresonant $B_s^0 \to J/\psi K^+ K^-$ decays is estimated by generating two sets of pseudo-experiments, one with just $B_s^0 \to J/\psi \phi(1020)$ events and one with a fraction of S-wave events based on the measured S-wave fraction and its uncertainty. The difference in the average of the measured lifetimes of these two samples is $0.74\,\mu$m, which is used to correct the measured lifetime. The systematic uncertainty associated with this correction is obtained by taking the difference in quadrature between the standard deviation of the distribution of lifetime results from the pseudo-experiments with and without the S-wave contribution.

7. PV selection in the $B_c^+ \to J/\psi \pi^+$ channel
   From the multiple reconstructed PVs in an event, one is selected to compute the ct value of the candidate. Two alternative methods to select the PV position are studied: using the centre of the beamspot and selecting the PV with the largest sum of track p_T. While all three methods are found to be effective and unbiased, there were small differences, and the maximum deviation with respect to the nominal choice is taken as the systematic uncertainty. The B^+ and B_c^+ primary vertex choices were changed coherently.

8. Detector alignment in the $B_c^+ \to J/\psi \pi^+$ channel
   Possible effects on the lifetime due to uncertainties in the detector alignment [29] are investigated for each decay topology using 20 different simulated samples with distorted geometries. These distortions include expansions in the radial and longitudinal dimensions, rotations, twists, offsets, etc. The amount of misalignment is chosen such that it is large enough to be detected and corrected by the alignment procedure. The standard deviation of the lifetimes for the tested scenarios is taken as the sys-

tematic uncertainty from this source. The B^+ and B_c^+ geometries were changed coherently.

9. Absolute ct accuracy in the B_s^0, B^0, and Λ_b^0 lifetime measurements

   The lifetime of the most statistically precise mode ($B^+ \to J/\psi K^+$) is used to validate the accuracy of the simulation and various detector calibrations. The difference between our measurement of $490.9 \pm 0.8\,\mu m$ (statistical uncertainty only) and the world-average value of $491.1 \pm 1.2\,\mu m$ [5] is $0.2 \pm 1.4\,\mu m$. This implies a limit to the validation of $1.4/491 = 0.3\%$. Four systematic effects that we expect to be included were checked independently. The systematic uncertainties from PV selection and detector alignment were found to be $0.7\,\mu m$ and 0.3–$0.7\,\mu m$, respectively. Varying the efficiency functional form changed the lifetimes by 0.3–$0.6\,\mu m$, while varying σ_{ct} by factors of 0.5 and 2.0 resulted in lifetime differences of no more than $0.2\,\mu m$. As the sum in quadrature of these uncertainties is less than that obtained from the B^+ lifetime comparison, we assign a value of 0.3% as the systematic uncertainty for the absolute ct accuracy.

8 Lifetime measurement results

Our final results for the B^0, B_s^0, and Λ_b^0 hadron lifetimes are:

$$c\tau_{B^0 \to J/\psi K^*(892)^0} = 453.0 \pm 1.6\,(\text{stat}) \pm 1.8\,(\text{syst})\,\mu m, \tag{12}$$

$$c\tau_{B^0 \to J/\psi K_S^0} = 457.8 \pm 2.7\,(\text{stat}) \pm 2.8\,(\text{syst})\,\mu m, \tag{13}$$

$$c\tau_{B_s^0 \to J/\psi \pi^+\pi^-} = 502.7 \pm 10.2\,(\text{stat}) \pm 3.4\,(\text{syst})\,\mu m, \tag{14}$$

$$c\tau_{B_s^0 \to J/\psi \phi(1020)} = 443.9 \pm 2.0\,(\text{stat}) \pm 1.5\,(\text{syst})\,\mu m, \tag{15}$$

$$c\tau_{\Lambda_b^0} = 442.9 \pm 8.2\,(\text{stat}) \pm 2.8\,(\text{syst})\,\mu m. \tag{16}$$

The value of the B_s^0 lifetime using the $J/\psi\phi(1020)$ decay has been corrected for the ct range and S-wave contamination effects described in Sect. 7. The lifetime ratios $\tau_{B_s^0}/\tau_{B^0}$ and $\tau_{\Lambda_b^0}/\tau_{B^0}$ have been determined using the decay channels $B^0 \to J/\psi K^*(892)^0$, $B_s^0 \to J/\psi\phi(1020)$, and $\Lambda_b^0 \to J/\psi\Lambda^0$. Including the statistical and correlated and uncorrelated systematic uncertainties, the results are:

$$\begin{aligned} &\tau_{\Lambda_b^0}/\tau_{B^0 \to J/\psi K^*(892)^0} \\ &= 0.978 \pm 0.018\,(\text{stat}) \pm 0.006\,(\text{syst}), \end{aligned} \tag{17}$$

$$\begin{aligned} &\tau_{\Lambda_b^0}/\tau_{B^0 \to J/\psi K^*(892)^0} \\ &= 0.978 \pm 0.018\,(\text{stat}) \pm 0.006\,(\text{syst}), \end{aligned} \tag{18}$$

These ratios are compatible with the current world-average values.

The measured lifetimes for the B^0 meson in the two different channels are in agreement. Combining the two results,

including the statistical and the correlated and uncorrelated systematic uncertainties, gives $c\tau_{B^0} = 454.1 \pm 1.4\,(\text{stat}) \pm 1.7\,(\text{syst})\,\mu m$. The lifetime measurements can also be used to estimate Γ_d and $\Delta\Gamma_d$ [6]. In the standard model, the effective lifetimes of the two B^0 decay modes can be written as:

$$\tau_{B^0 \to J/\psi K^*(892)^0} = \frac{1}{\Gamma_d}\left(\frac{1}{1 - y_d^2}\right)\left(\frac{1 + 2\cos(2\beta)y_d + y_d^2}{1 + \cos(2\beta)y_d}\right), \tag{19}$$

$$\tau_{B^0 \to J/\psi K_S^0} = \frac{1}{\Gamma_d}\left(\frac{1 + y_d^2}{1 - y_d^2}\right), \tag{20}$$

where $y_d = \Delta\Gamma_d/2\Gamma_d$, and $\beta = (21.9 \pm 0.7)°$ [5] is one of the CKM unitarity triangle angles. Using our measured values for the two B^0 lifetimes, we fit for Γ_d and $\Delta\Gamma_d$ and use the values to determine $\Delta\Gamma_d/\Gamma_d$. The results are:

$$\Gamma_d = 0.662 \pm 0.003\,(\text{stat}) \pm 0.003\,(\text{syst})\,\text{ps}^{-1}, \tag{21}$$

$$\Delta\Gamma_d = 0.023 \pm 0.015\,(\text{stat}) \pm 0.016\,(\text{syst})\,\text{ps}^{-1}, \tag{22}$$

$$\Delta\Gamma_d/\Gamma_d = 0.034 \pm 0.023\,(\text{stat}) \pm 0.024\,(\text{syst}). \tag{23}$$

Neglecting CP violation in mixing, the measured $B_s^0 \to J/\psi\pi^+\pi^-$ lifetime can be translated into the width of the heavy B_s^0 mass eigenstate:

$$\Gamma_H = 1/\tau_{B_s^0} = 0.596 \pm 0.012\,(\text{stat}) \pm 0.004\,(\text{syst})\,\text{ps}^{-1}. \tag{24}$$

Solving for $c\tau_L$ from Eq. (4) gives

$$c\tau_L = \frac{1}{2}c\tau_{\text{eff}} + \sqrt{\frac{1}{4}(c\tau_{\text{eff}})^2 - \frac{|A_\perp|^2}{1 - |A_\perp|^2}c\tau_H(c\tau_H - c\tau_{\text{eff}})}. \tag{25}$$

Using the $B_s^0 \to J/\psi\pi^+\pi^-$ result in Eq. (14), the measured B_s^0 effective lifetime in Eq. (15), and the world-average value of the magnitude squared of the CP-odd amplitude $|A_\perp|^2 = 0.250 \pm 0.006$ [2], the lifetime of the light component is found to be $c\tau_L = 420.4 \pm 6.2\,\mu m$. The uncertainty includes all statistical and systematic uncertainties, taking into account the correlated uncertainties. The result is consistent with the world-average value of $423.6 \pm 1.8\,\mu m$ [5].

Our measured lifetimes for B^0, $B_s^0 \to J/\psi\phi(1020)$, and Λ_b^0 are compatible with the current world-average values [5] of 455.7 ± 1.2, 443.4 ± 3.6, and $440.7 \pm 3.0\,\mu m$, respectively. In addition, our measurement of the B_s^0 lifetime in the $B_s^0 \to J/\psi\pi^+\pi^-$ channel is in agreement with the results from CDF, LHCb, and D0: $510\,^{+36}_{-33}\,(\text{stat}) \pm 9\,(\text{syst})\,\mu m$ [30], $495.3 \pm 7.2\,(\text{stat}) \pm 7.2\,(\text{syst})\,\mu m$ [31], and $508 \pm 42\,(\text{stat}) \pm 16\,(\text{syst})\,\mu m$ [32], respectively.

Our final result for the B_c^+ lifetime using the $J/\psi \pi^+$ mode is:

$$c\tau_{B_c^+} = 162.3 \pm 7.8 \,(\text{stat}) \pm 4.2 \,(\text{syst}) \pm 0.1 \,(\tau_{B^+}) \,\mu\text{m}, \tag{26}$$

where the systematic uncertainty from the B^+ lifetime uncertainty [5] is quoted separately in the result. This measurement is in agreement with the world-average value $(152.0 \pm 2.7 \,\mu\text{m})$ [5]. Precise measurements of the B_c^+ lifetime allow tests of various theoretical models, which predict values ranging from 90 to 210 μm [33–36]. Furthermore, they provide new constraints on possible physics beyond the standard model from the observed anomalies in $B \to D^{(*)}\tau\nu$ decays [37].

9 Summary

The lifetimes of the B^0, B_s^0, Λ_b^0, and B_c^+ hadrons have been measured using fully reconstructed decays with a J/ψ meson. The data were collected by the CMS detector in proton–proton collision events at a centre-of-mass energy of 8 TeV, and correspond to an integrated luminosity of 19.7 fb^{-1}. The B^0 and B_s^0 meson lifetimes have each been measured in two channels: $J/\psi K^*(892)^0$, $J/\psi K_S^0$ for B^0 and $J/\psi \pi^+\pi^-$, $J/\psi \phi(1020)$ for B_s^0. The precision from each channel is as good as or better than previous measurements in the respective channel. The B^0 lifetime results are used to obtain an average lifetime and to measure the decay width difference between the two mass eigenstates. The B_s^0 lifetime results are used to obtain the lifetimes of the heavy and light B_s^0 mass eigenstates. The precision of the Λ_b^0 lifetime measurement is also as good as any previous measurement in the $J/\psi \Lambda^0$ channel. The measured B_c^+ meson lifetime is in agreement with the results from LHCb and significantly more precise than the CDF and D0 measurements. All measured lifetimes are compatible with the current world-average values.

References

1. A. Lenz, Lifetimes and heavy quark expansion. Int. J. Mod. Phys. A **30**, 1543005 (2015). https://doi.org/10.1142/S0217751X15430058
2. Particle Data Group, C. Patrignani et al., Review of particle physics. Chin. Phys. C **40**, 100001 (2016). https://doi.org/10.1088/1674-1137/40/10/100001
3. CMS Collaboration, The CMS experiment at the CERN LHC. JINST **3**, S08004 (2008). https://doi.org/10.1088/1748-0221/3/08/S08004
4. R. Fleischer, R. Knegjens, Effective lifetimes of B_s decays and their constraints on the B_s^0-$\bar{B}_s^0$ mixing parameters. Eur. Phys. J. C **71**, 1789 (2011). https://doi.org/10.1140/epjc/s10052-011-1789-9. arXiv:1109.5115
5. Heavy Flavor Averaging Group, Y. Amhis et al., Averages of b-hadron, c-hadron, and τ-lepton properties as of summer 2016. Eur. Phys. J. C **77**, 895 (2017). https://doi.org/10.1140/epjc/s10052-017-5058-4, arXiv:1612.07233
6. T. Gershon, $\delta\gamma\_d$: a forgotten null test of the standard model. J. Phys. G **38** (2011). https://doi.org/10.1088/0954-3899/38/1/015007, arXiv:1007.5135
7. LHCb Collaboration, Analysis of the resonant components in $\bar{B}^0\_s \to J/\psi\pi^+\pi^-$. Phys. Rev. D **86**, 052006 (2012). https://doi.org/10.1103/PhysRevD.86.052006, arXiv:1301.5347

8. LHCb Collaboration, Measurement of resonant and CP components in $\overline{B}^0$_s $\rightarrow J/\psi\pi^+\pi^-$. Phys. Rev. D **89**, 092006 (2014). https://doi.org/10.1103/PhysRevD.89.092006, arXiv:1402.6248

9. CMS Collaboration, Measurement of the CP-violating weak phase ϕ_s and the decay width difference $\Delta\Gamma$_s using the B^0_s $\rightarrow J/\psi\phi(1020)$ decay channel in pp collisions at $\sqrt{s} = 8$TeV. Phys. Lett. B **757**, 97 (2016). https://doi.org/10.1016/j.physletb.2016.03.046, arXiv:1507.07527

10. V.V. Kiselev, Exclusive decays and lifetime of B_c meson in QCD sum rules (2002). arXiv:hep-ph/0211021

11. LHCb Collaboration, "Measurement of the B_c$^+$ meson lifetime using B_c$^+$ $\rightarrow J/\psi\mu^+\nu$_$\mu$X decays", Eur. Phys. J. C **74**, 2839, (2014) https://doi.org/10.1140/epjc/s10052-014-2839-x, arXiv:1401.6932

12. LHCb Collaboration, Measurement of the lifetime of the B_c$^+$ meson using the B_c$^+$ $\rightarrow J/\psi\pi^+$ decay mode. Phys. Lett. B **742**, 29 (2015). https://doi.org/10.1016/j.physletb.2015.01.010, arXiv:1411.6899

13. CDF Collaboration, Observation of the B_c meson in p$\overline{p}$ collisions at $\sqrt{s} = 1.8$TeV. Phys. Rev. Lett. **81**, 2432 (1998). https://doi.org/10.1103/PhysRevLett.81.2432, arXiv:hep-ex/9805034

14. CDF Collaboration, Measurement of the B_c$^+$ meson lifetime using the decay mode B_c$^+$ $\rightarrow J/\psi$e$^\pm\nu$_e. Phys. Rev. Lett. **97**, 012002 (2006). https://doi.org/10.1103/PhysRevLett.97.012002, arXiv:hep-ex/0603027

15. D0 Collaboration, Measurement of the lifetime of the B$^\pm$_c meson in the semileptonic decay channel. Phys. Rev. Lett. **102**, 092001 (2009). https://doi.org/10.1103/PhysRevLett.102.092001, arXiv:0805.2614

16. C.D.F. Collaboration, Measurement of the B_c$^-$ meson lifetime in the decay B_c$^-$ $\rightarrow J/\psi\pi^-$. Phys. Rev. D **87**, 011101 (2013). https://doi.org/10.1103/PhysRevD.87.011101. arXiv:1210.2366

17. CMS Collaboration, Description and performance of track and primary-vertex reconstruction with the CMS tracker. JINST **9**, P10009 (2014). https://doi.org/10.1088/1748-0221/9/10/P10009,arXiv:1405.6569

18. CMS Collaboration, The CMS trigger system. JINST **12**, P01020 (2017). https://doi.org/10.1088/1748-0221/12/01/P01020, arXiv:1609.02366

19. T. Sjöstrand, S. Mrenna, P.Z. Skands, PYTHIA 6.4 physics and manual. JHEP **05**, 026 (2006). https://doi.org/10.1088/1126-6708/2006/05/026. arXiv:hep-ph/0603175

20. C. Chang, C. Driouchi, P. Eerola, X. Wu, BCVEGPY: an event generator for hadronic production of the B_c meson. Comput. Phys. Commun. **159**, 192 (2004). https://doi.org/10.1016/j.cpc.2004.02.005. arXiv:hep-ph/0309120

21. C. Chang, J. Wang, X. Wu, BCVEGPY2.0: an upgraded version of the generator BCVEGPY with the addition of hadroproduction of the P-wave B_c states. Comput. Phys. Commun. **174**, 241 (2006). https://doi.org/10.1016/j.cpc.2005.09.008. arXiv:hep-ph/0504017

22. D.J. Lange, The EvtGen particle decay simulation package. Nucl. Instrum. Methods A **462**, 152 (2001). https://doi.org/10.1016/S0168-9002(01)00089-4

23. P. Golonka, Z. Wąs, PHOTOS Monte Carlo: a precision tool for QED corrections in Z and W decays. Eur. Phys. J. C **45**, 97 (2006). https://doi.org/10.1140/epjc/s2005-02396-4. arXiv:hep-ph/0506026

24. GEANT4 Collaboration, GEANT4—a simulation toolkit. Nucl. Instrum. Methods A **506**, 250 (2003). https://doi.org/10.1016/S0168-9002(03)01368-8

25. CMS Collaboration, Performance of CMS muon reconstruction in pp collision events at $\sqrt{s} = 7$TeV. JINST **7**, P10002 (2012). https://doi.org/10.1088/1748-0221/7/10/P10002, arXiv:1206.4071

26. A.S. Dighe, I. Dunietz, R. Fleischer, Extracting CKM phases and B_s $-$ $\overline{B}$_s mixing parameters from angular distributions of nonleptonic B decays. Eur. Phys. J. C **6**, 647 (1999). https://doi.org/10.1007/s100529800954. arXiv:hep-ph/9804253

27. LHCb Collaboration, First observation of the decay B$^+$_c $\rightarrow J/\psi$K$^+$. JHEP **09**, 075 (2013). https://doi.org/10.1007/JHEP09(2013)075, arXiv:1306.6723

28. M.J. Oreglia, A study of the reactions $\psi' \rightarrow \gamma\gamma\psi$. Ph.D. Thesis, Stanford University (1980). SLAC Report SLAC-R-236, see Appendix D

29. CMS Collaboration, Alignment of the CMS tracker with LHC and cosmic ray data. JINST **9**, P06009 (2014). https://doi.org/10.1088/1748-0221/9/06/P06009, arXiv:1403.2286

30. CDF Collaboration, Measurement of branching ratio and B^0_s lifetime in the decay B^0_s $\rightarrow J/\psi$f_0(980) at CDF. Phys. Rev. D **84**, 052012 (2011). https://doi.org/10.1103/PhysRevD.84.052012, arXiv:1106.3682

31. LHCb Collaboration, Measurement of CP violation and the B^0_s meson decay width difference with B^0_s $\rightarrow J/\psi$K$^+$K$^-$ and B^0_s $\rightarrow J/\psi\pi^+\pi^-$ decays. Phys. Rev. D **87**, 112010 (2013). https://doi.org/10.1103/PhysRevD.87.112010, arXiv:1304.2600

32. D0 Collaboration, B^0_s lifetime measurement in the CP-odd decay channel B^0_s $\rightarrow J/\psi$f_0(980), Phys. Rev. D **94**, 012001 (2016). https://doi.org/10.1103/PhysRevD.94.012001, arXiv:1603.01302

33. C.-H. Chang, S.-L. Chen, T.-F. Feng, X.-Q. Li, Lifetime of the B_c meson and some relevant problems. Phys. Rev. D **64**, 014003 (2001). https://doi.org/10.1103/PhysRevD.64.014003. arXiv:hep-ph/0007162

34. M. Beneke, G. Buchalla, B_c meson lifetime. Phys. Rev. D **53**, 4991 (1996). https://doi.org/10.1103/PhysRevD.53.4991. arXiv:hep-ph/9601249

35. AYu. Anisimov, I.M. Narodetskii, C. Semay, B. Silvestre-Brac, The B_c meson lifetime in the light-front constituent quark model. Phys. Lett. B **452**, 129 (1999). https://doi.org/10.1016/S0370-2693(99)00273-7. arXiv:hep-ph/9812514

36. V.V. Kiselev, A.E. Kovalsky, A.K. Likhoded, "Decays and lifetime of B_c in QCD sum rules", in 5th International Workshop on Heavy Quark Physics, Dubna, Russia, April 6-8, (2000). arXiv:hep-ph/0006104

37. R. Alonso, B. Grinstein, J. Martin Camalich, Lifetime of B_c$^-$ constrains explanations for anomalies in B $\rightarrow$ D$^{(*)}\tau\nu$. Phys. Rev. Lett. **118**, 081802 (2017). https://doi.org/10.1103/PhysRevLett.118.081802. arXiv:1611.06676

CMS Collaboration

Yerevan Physics Institute, Yerevan, Armenia
A. M. Sirunyan, A. Tumasyan

Institut für Hochenergiephysik, Wien, Austria
W. Adam, F. Ambrogi, E. Asilar, T. Bergauer, J. Brandstetter, E. Brondolin, M. Dragicevic, J. Erö, M. Flechl, M. Friedl, R. Frühwirth[1], V. M. Ghete, J. Grossmann, J. Hrubec, M. Jeitler[1], A. König, N. Krammer, I. Krätschmer, D. Liko, T. Madlener, I. Mikulec, E. Pree, N. Rad, H. Rohringer, J. Schieck[1], R. Schöfbeck, M. Spanring, D. Spitzbart, W. Waltenberger, J. Wittmann, C.-E. Wulz[1], M. Zarucki

Institute for Nuclear Problems, Minsk, Belarus
Y. Dydyshka, V. Mossolov, J. Suarez Gonzalez

Universiteit Antwerpen, Antwerpen, Belgium
E. A. De Wolf, D. Di Croce, X. Janssen, J. Lauwers, H. Van Haevermaet, P. Van Mechelen, N. Van Remortel

Vrije Universiteit Brussel, Brussels, Belgium
S. Abu Zeid, F. Blekman, J. D'Hondt, I. De Bruyn, J. De Clercq, K. Deroover, G. Flouris, D. Lontkovskyi, S. Lowette, S. Moortgat, L. Moreels, Q. Python, K. Skovpen, S. Tavernier, W. Van Doninck, P. Van Mulders, I. Van Parijs

Université Libre de Bruxelles, Brussels, Belgium
D. Beghin, H. Brun, B. Clerbaux, G. De Lentdecker, H. Delannoy, B. Dorney, G. Fasanella, L. Favart, R. Goldouzian, A. Grebenyuk, G. Karapostoli, T. Lenzi, J. Luetic, T. Maerschalk, A. Marinov, A. Randle-conde, T. Seva, C. Vander Velde, P. Vanlaer, D. Vannerom, R. Yonamine, F. Zenoni, F. Zhang[2]

Ghent University, Ghent, Belgium
A. Cimmino, T. Cornelis, D. Dobur, A. Fagot, M. Gul, I. Khvastunov, D. Poyraz, C. Roskas, S. Salva, M. Tytgat, W. Verbeke, N. Zaganidis

Université Catholique de Louvain, Louvain-la-Neuve, Belgium
H. Bakhshiansohi, O. Bondu, S. Brochet, G. Bruno, C. Caputo, A. Caudron, P. David, S. De Visscher, C. Delaere, M. Delcourt, B. Francois, A. Giammanco, M. Komm, G. Krintiras, V. Lemaitre, A. Magitteri, A. Mertens, M. Musich, K. Piotrzkowski, L. Quertenmont, A. Saggio, M. Vidal Marono, S. Wertz, J. Zobec

Université de Mons, Mons, Belgium
N. Beliy

Centro Brasileiro de Pesquisas Fisicas, Rio de Janeiro, Brazil
W. L. AldáJúnior, F. L. Alves, G. A. Alves, L. Brito, M. Correa Martins Jr., C. Hensel, A. Moraes, M. E. Pol, P. Rebello Teles

Universidade do Estado do Rio de Janeiro, Rio de Janeiro, Brazil
E. Belchior Batista Das Chagas, W. Carvalho, J. Chinellato[3], E. Coelho, E. M. Da Costa, G. G. Da Silveira[4], D. De Jesus Damiao, S. Fonseca De Souza, L. M. Huertas Guativa, H. Malbouisson, M. Melo De Almeida, C. Mora Herrera, L. Mundim, H. Nogima, L. J. Sanchez Rosas, A. Santoro, A. Sznajder, M. Thiel, E. J. Tonelli Manganote[3], F. Torres Da Silva De Araujo, A. Vilela Pereira

Universidade Estadual Paulista[a], Universidade Federal do ABC[b], São Paulo, Brazil
S. Ahuja[a], C. A. Bernardes[a], T. R. Fernandez Perez Tomei[a], E. M. Gregores[b], P. G. Mercadante[b], S. F. Novaes[a], Sandra S. Padula[a], D. Romero Abad[b], J. C. Ruiz Vargas[a]

Institute for Nuclear Research and Nuclear Energy, Bulgarian Academy of Sciences, Sofia, Bulgaria
A. Aleksandrov, R. Hadjiiska, P. Iaydjiev, M. Misheva, M. Rodozov, M. Shopova, G. Sultanov

University of Sofia, Sofia, Bulgaria
A. Dimitrov, I. Glushkov, L. Litov, B. Pavlov, P. Petkov

Beihang University, Beijing, China
W. Fang[5], X. Gao[5], L. Yuan

Institute of High Energy Physics, Beijing, China
M. Ahmad, J. G. Bian, G. M. Chen, H. S. Chen, M. Chen, Y. Chen, C. H. Jiang, D. Leggat, H. Liao, Z. Liu, F. Romeo, S. M. Shaheen, A. Spiezia, J. Tao, C. Wang, Z. Wang, E. Yazgan, H. Zhang, S. Zhang, J. Zhao

State Key Laboratory of Nuclear Physics and Technology, Peking University, Beijing, China
Y. Ban, G. Chen, Q. Li, S. Liu, Y. Mao, S. J. Qian, D. Wang, Z. Xu

Universidad de Los Andes, Bogotá, Colombia
C. Avila, A. Cabrera, L. F. Chaparro Sierra, C. Florez, C. F. González Hernández, J. D. Ruiz Alvarez

University of Split, Faculty of Electrical Engineering, Mechanical Engineering and Naval Architecture, Split, Croatia
B. Courbon, N. Godinovic, D. Lelas, I. Puljak, P. M. Ribeiro Cipriano, T. Sculac

University of Split, Faculty of Science, Split, Croatia
Z. Antunovic, M. Kovac

Institute Rudjer Boskovic, Zagreb, Croatia
V. Brigljevic, D. Ferencek, K. Kadija, B. Mesic, A. Starodumov[6], T. Susa

University of Cyprus, Nicosia, Cyprus
M. W. Ather, A. Attikis, G. Mavromanolakis, J. Mousa, C. Nicolaou, F. Ptochos, P. A. Razis, H. Rykaczewski

Charles University, Prague, Czech Republic
M. Finger[7], M. Finger Jr.[7]

Universidad San Francisco de Quito, Quito, Ecuador
E. Carrera Jarrin

Academy of Scientific Research and Technology of the Arab Republic of Egypt, Egyptian Network of High Energy Physics, Cairo, Egypt
Y. Assran[8,9], S. Elgammal[9], A. Mahrous[10]

National Institute of Chemical Physics and Biophysics, Tallinn, Estonia
R. K. Dewanjee, M. Kadastik, L. Perrini, M. Raidal, A. Tiko, C. Veelken

Department of Physics, University of Helsinki, Helsinki, Finland
P. Eerola, H. Kirschenmann, J. Pekkanen, M. Voutilainen

Helsinki Institute of Physics, Helsinki, Finland
T. Järvinen, V. Karimäki, R. Kinnunen, T. Lampén, K. Lassila-Perini, S. Lehti, T. Lindén, P. Luukka, E. Tuominen, J. Tuominiemi

Lappeenranta University of Technology, Lappeenranta, Finland
J. Talvitie, T. Tuuva

IRFU, CEA, Université Paris-Saclay, Gif-sur-Yvette, France
M. Besancon, F. Couderc, M. Dejardin, D. Denegri, J. L. Faure, F. Ferri, S. Ganjour, S. Ghosh, A. Givernaud, P. Gras, G. Hamel de Monchenault, P. Jarry, I. Kucher, C. Leloup, E. Locci, M. Machet, J. Malcles, G. Negro, J. Rander, A. Rosowsky, M. Ö. Sahin, M. Titov

Laboratoire Leprince-Ringuet, Ecole polytechnique, CNRS/IN2P3, Université Paris-Saclay, Palaiseau, France
A. Abdulsalam, C. Amendola, I. Antropov, S. Baffioni, F. Beaudette, P. Busson, L. Cadamuro, C. Charlot, R. Granier de Cassagnac, M. Jo, S. Lisniak, A. Lobanov, J. Martin Blanco, M. Nguyen, C. Ochando, G. Ortona, P. Paganini, P. Pigard, R. Salerno, J. B. Sauvan, Y. Sirois, A. G. Stahl Leiton, T. Strebler, Y. Yilmaz, A. Zabi, A. Zghiche

Université de Strasbourg, CNRS, IPHC UMR 7178, 67000 Strasbourg, France
J.-L. Agram[11], J. Andrea, D. Bloch, J.-M. Brom, M. Buttignol, E. C. Chabert, N. Chanon, C. Collard, E. Conte[11], X. Coubez, J.-C. Fontaine[11], D. Gelé, U. Goerlach, M. Jansová, A.-C. Le Bihan, N. Tonon, P. Van Hove

Centre de Calcul de l'Institut National de Physique Nucleaire et de Physique des Particules, CNRS/IN2P3, Villeurbanne, France

S. Gadrat

Université de Lyon, Université Claude Bernard Lyon 1, CNRS-IN2P3, Institut de Physique Nucléaire de Lyon, Villeurbanne, France

S. Beauceron, C. Bernet, G. Boudoul, R. Chierici, D. Contardo, P. Depasse, H. ElMamouni, J. Fay, L. Finco, S. Gascon, M. Gouzevitch, G. Grenier, B. Ille, F. Lagarde, I. B. Laktineh, M. Lethuillier, L. Mirabito, A. L. Pequegnot, S. Perries, A. Popov[12], V. Sordini, M. Vander Donckt, S. Viret

Georgian Technical University, Tbilisi, Georgia

T. Toriashvili[13]

Tbilisi State University, Tbilisi, Georgia

I. Bagaturia[14]

RWTH Aachen University, I. Physikalisches Institut, Aachen, Germany

C. Autermann, L. Feld, M. K. Kiesel, K. Klein, M. Lipinski, M. Preuten, C. Schomakers, J. Schulz, T. Verlage, V. Zhukov[12]

RWTH Aachen University, III. Physikalisches Institut A, Aachen, Germany

A. Albert, E. Dietz-Laursonn, D. Duchardt, M. Endres, M. Erdmann, S. Erdweg, T. Esch, R. Fischer, A. Güth, M. Hamer, T. Hebbeker, C. Heidemann, K. Hoepfner, S. Knutzen, M. Merschmeyer, A. Meyer, P. Millet, S. Mukherjee, T. Pook, M. Radziej, H. Reithler, M. Rieger, F. Scheuch, D. Teyssier, S. Thüer

RWTH Aachen University, III. Physikalisches Institut B, Aachen, Germany

G. Flügge, B. Kargoll, T. Kress, A. Künsken, J. Lingemann, T. Müller, A. Nehrkorn, A. Nowack, C. Pistone, O. Pooth, A. Stahl[15]

Deutsches Elektronen-Synchrotron, Hamburg, Germany

M. Aldaya Martin, T. Arndt, C. Asawatangtrakuldee, K. Beernaert, O. Behnke, U. Behrens, A. Bermúdez Martínez, A. A. Bin Anuar, K. Borras[16], V. Botta, A. Campbell, P. Connor, C. Contreras-Campana, F. Costanza, C. Diez Pardos, G. Eckerlin, D. Eckstein, T. Eichhorn, E. Eren, E. Gallo[17], J. Garay Garcia, A. Geiser, A. Gizhko, J. M. Grados Luyando, A. Grohsjean, P. Gunnellini, M. Guthoff, A. Harb, J. Hauk, M. Hempel[18], H. Jung, A. Kalogeropoulos, M. Kasemann, J. Keaveney, C. Kleinwort, I. Korol, D. Krücker, W. Lange, A. Lelek, T. Lenz, J. Leonard, K. Lipka, W. Lohmann[18], R. Mankel, I.-A. Melzer-Pellmann, A. B. Meyer, G. Mittag, J. Mnich, A. Mussgiller, E. Ntomari, D. Pitzl, A. Raspereza, B. Roland, M. Savitskyi, P. Saxena, R. Shevchenko, S. Spannagel, N. Stefaniuk, G. P. Van Onsem, R. Walsh, Y. Wen, K. Wichmann, C. Wissing, O. Zenaiev

University of Hamburg, Hamburg, Germany

R. Aggleton, S. Bein, V. Blobel, M. Centis Vignali, T. Dreyer, E. Garutti, D. Gonzalez, J. Haller, A. Hinzmann, M. Hoffmann, A. Karavdina, R. Klanner, R. Kogler, N. Kovalchuk, S. Kurz, T. Lapsien, I. Marchesini, D. Marconi, M. Meyer, M. Niedziela, D. Nowatschin, F. Pantaleo[15], T. Peiffer, A. Perieanu, C. Scharf, P. Schleper, A. Schmidt, S. Schumann, J. Schwandt, J. Sonneveld, H. Stadie, G. Steinbrück, F. M. Stober, M. Stöver, H. Tholen, D. Troendle, E. Usai, L. Vanelderen, A. Vanhoefer, B. Vormwald

Institut für Experimentelle Kernphysik, Karlsruhe, Germany

M. Akbiyik, C. Barth, S. Baur, E. Butz, R. Caspart, T. Chwalek, F. Colombo, W. De Boer, A. Dierlamm, B. Freund, R. Friese, M. Giffels, D. Haitz, F. Hartmann[15], S. M. Heindl, U. Husemann, F. Kassel[15], S. Kudella, H. Mildner, M. U. Mozer, Th. Müller, M. Plagge, G. Quast, K. Rabbertz, M. Schröder, I. Shvetsov, G. Sieber, H. J. Simonis, R. Ulrich, S. Wayand, M. Weber, T. Weiler, S. Williamson, C. Wöhrmann, R. Wolf

Institute of Nuclear and Particle Physics (INPP), NCSR Demokritos, Aghia Paraskevi, Greece

G. Anagnostou, G. Daskalakis, T. Geralis, V. A. Giakoumopoulou, A. Kyriakis, D. Loukas, I. Topsis-Giotis

National and Kapodistrian University of Athens, Athens, Greece

G. Karathanasis, S. Kesisoglou, A. Panagiotou, N. Saoulidou

National Technical University of Athens, Athens, Greece

K. Kousouris

University of Ioánnina, Ioannina, Greece

I. Evangelou, C. Foudas, P. Kokkas, S. Mallios, N. Manthos, I. Papadopoulos, E. Paradas, J. Strologas, F. A. Triantis

MTA-ELTE Lendület CMS Particle and Nuclear Physics Group, Eötvös Loránd University, Budapest, Hungary

M. Csanad, N. Filipovic, G. Pasztor, O. Surányi, G. I. Veres[19]

Wigner Research Centre for Physics, Budapest, Hungary

G. Bencze, C. Hajdu, D. Horvath[20], Á. Hunyadi, F. Sikler, V. Veszpremi, A. J. Zsigmond

Institute of Nuclear Research ATOMKI, Debrecen, Hungary

N. Beni, S. Czellar, J. Karancsi[21], A. Makovec, J. Molnar, Z. Szillasi

Institute of Physics, University of Debrecen, Debrecen, Hungary

M. Bartók[19], P. Raics, Z. L. Trocsanyi, B. Ujvari

Indian Institute of Science (IISc), Bangalore, India

S. Choudhury, J. R. Komaragiri

National Institute of Science Education and Research, Bhubaneswar, India

S. Bahinipati[22], S. Bhowmik, P. Mal, K. Mandal, A. Nayak[23], D. K. Sahoo[22], N. Sahoo, S. K. Swain

Panjab University, Chandigarh, India

S. Bansal, S. B. Beri, V. Bhatnagar, R. Chawla, N. Dhingra, A. K. Kalsi, A. Kaur, M. Kaur, S. Kaur, R. Kumar, P. Kumari, A. Mehta, J. B. Singh, G. Walia

University of Delhi, Delhi, India

Ashok Kumar, Aashaq Shah, A. Bhardwaj, S. Chauhan, B. C. Choudhary, R. B. Garg, S. Keshri, A. Kumar, S. Malhotra, M. Naimuddin, K. Ranjan, R. Sharma

Saha Institute of Nuclear Physics, HBNI, Kolkata, India

R. Bhardwaj, R. Bhattacharya, S. Bhattacharya, U. Bhawandeep, S. Dey, S. Dutt, S. Dutta, S. Ghosh, N. Majumdar, A. Modak, K. Mondal, S. Mukhopadhyay, S. Nandan, A. Purohit, A. Roy, D. Roy, S. Roy Chowdhury, S. Sarkar, M. Sharan, S. Thakur

Indian Institute of Technology Madras, Madras, India

P. K. Behera

Bhabha Atomic Research Centre, Mumbai, India

R. Chudasama, D. Dutta, V. Jha, V. Kumar, A. K. Mohanty[15], P. K. Netrakanti, L. M. Pant, P. Shukla, A. Topkar

Tata Institute of Fundamental Research-A, Mumbai, India

T. Aziz, S. Dugad, B. Mahakud, S. Mitra, G. B. Mohanty, N. Sur, B. Sutar

Tata Institute of Fundamental Research-B, Mumbai, India

S. Banerjee, S. Bhattacharya, S. Chatterjee, P. Das, M. Guchait, Sa. Jain, S. Kumar, M. Maity[24], G. Majumder, K. Mazumdar, T. Sarkar[24], N. Wickramage[25]

Indian Institute of Science Education and Research (IISER), Pune, India

S. Chauhan, S. Dube, V. Hegde, A. Kapoor, K. Kothekar, S. Pandey, A. Rane, S. Sharma

Institute for Research in Fundamental Sciences (IPM), Tehran, Iran

S. Chenarani[26], E. Eskandari Tadavani, S. M. Etesami[26], M. Khakzad, M. Mohammadi Najafabadi, M. Naseri, S. Paktinat Mehdiabadi[27], F. Rezaei Hosseinabadi, B. Safarzadeh[28], M. Zeinali

University College Dublin, Dublin, Ireland

M. Felcini, M. Grunewald

INFN Sezione di Bari^a, Università di Bari^b, Politecnico di Bari^c, Bari, Italy

M. Abbrescia^{a,b}, C. Calabria^{a,b}, A. Colaleo^a, D. Creanza^{a,c}, L. Cristella^{a,b}, N. De Filippis^{a,c}, M. De Palma^{a,b}, F. Errico^{a,b}, L. Fiore^a, G. Iaselli^{a,c}, S. Lezki^{a,b}, G. Maggi^{a,c}, M. Maggi^a, G. Miniello^{a,b}, S. My^{a,b}, S. Nuzzo^{a,b}, A. Pompili^{a,b}, G. Pugliese^{a,c}, R. Radogna^a, A. Ranieri^a, G. Selvaggi^{a,b}, A. Sharma^a, L. Silvestris^{a,15}, R. Venditti^a, P. Verwilligen^a

INFN Sezione di Bologna[a], Università di Bologna[b], Bologna, Italy

G. Abbiendi[a], C. Battilana[a,b], D. Bonacorsi[a,b], L. Borgonovi[a,b], S. Braibant-Giacomelli[a,b], R. Campanini[a,b], P. Capiluppi[a,b], A. Castro[a,b], F. R. Cavallo[a], S. S. Chhibra[a], G. Codispoti[a,b], M. Cuffiani[a,b], G. M. Dallavalle[a], F. Fabbri[a], A. Fanfani[a,b], D. Fasanella[a,b], P. Giacomelli[a], C. Grandi[a], L. Guiducci[a,b], S. Marcellini[a], G. Masetti[a], A. Montanari[a], F. L. Navarria[a,b], A. Perrotta[a], A. M. Rossi[a,b], T. Rovelli[a,b], G. P. Siroli[a,b], N. Tosi[a]

INFN Sezione di Catania[a], Università di Catania[b], Catania, Italy

S. Albergo[a,b], S. Costa[a,b], A. Di Mattia[a], F. Giordano[a,b], R. Potenza[a,b], A. Tricomi[a,b], C. Tuve[a,b]

INFN Sezione di Firenze[a], Università di Firenze[b], Florence, Italy

G. Barbagli[a], K. Chatterjee[a,b], V. Ciulli[a,b], C. Civinini[a], R. D'Alessandro[a,b], E. Focardi[a,b], P. Lenzi[a,b], M. Meschini[a], S. Paoletti[a], L. Russo[a,29], G. Sguazzoni[a], D. Strom[a], L. Viliani[a,b,15]

INFN Laboratori Nazionali di Frascati, Frascati, Italy

L. Benussi, S. Bianco, F. Fabbri, D. Piccolo, F. Primavera[15]

INFN Sezione di Genova[a], Università di Genova[b], Genoa, Italy

V. Calvelli[a,b], F. Ferro[a], E. Robutti[a], S. Tosi[a,b]

INFN Sezione di Milano-Bicocca[a], Università di Milano-Bicocca[b], Milan, Italy

A. Benaglia[a], L. Brianza[a,b], F. Brivio[a,b], V. Ciriolo[a,b], M. E. Dinardo[a,b], P. Dini[a], S. Fiorendi[a,b], S. Gennai[a], A. Ghezzi[a,b], P. Govoni[a,b], M. Malberti[a,b], S. Malvezzi[a], R. A. Manzoni[a,b], D. Menasce[a], L. Moroni[a], M. Paganoni[a,b], K. Pauwels[a,b], D. Pedrini[a], S. Pigazzini[a,b,30], S. Ragazzi[a,b], N. Redaelli[a], T. Tabarelli de Fatis[a,b]

INFN Sezione di Napoli[a], Università di Napoli 'Federico II' [b], Naples , Italy, Università della Basilicata[c], Potenza, Italy, Università G. Marconi[d], Rome, Italy

S. Buontempo[a], N. Cavallo[a,c], S. Di Guida[a,d,15], F. Fabozzi[a,c], F. Fienga[a,b], A. O. M. Iorio[a,b], W. A. Khan[a], L. Lista[a], S. Meola[a,d,15], P. Paolucci[a,15], C. Sciacca[a,b], F. Thyssen[a]

INFN Sezione di Padova[a], Università di Padova[b], Padova, Italy, Università di Trento[c], Trento, Italy

P. Azzi[a], L. Benato[a,b], D. Bisello[a,b], A. Boletti[a,b], R. Carlin[a,b], A. Carvalho Antunes De Oliveira[a,b], P. Checchia[a], M. Dall'Osso[a,b], P. De Castro Manzano[a], T. Dorigo[a], U. Dosselli[a], F. Gasparini[a,b], U. Gasparini[a,b], A. Gozzelino[a], S. Lacaprara[a], P. Lujan, M. Margoni[a,b], A. T. Meneguzzo[a,b], M. Passaseo[a], M. Pegoraro[a], N. Pozzobon[a,b], P. Ronchese[a,b], R. Rossin[a,b], F. Simonetto[a,b], M. Zanetti[a,b], G. Zumerle[a,b]

INFN Sezione di Pavia[a], Università di Pavia[b], Pavia, Italy

A. Braghieri[a], A. Magnani[a], P. Montagna[a,b], S. P. Ratti[a,b], V. Re[a], M. Ressegotti[a,b], C. Riccardi[a,b], P. Salvini[a], I. Vai[a,b], P. Vitulo[a,b]

INFN Sezione di Perugia[a], Università di Perugia[b], Perugia, Italy

L. Alunni Solestizi[a,b], M. Biasini[a,b], G. M. Bilei[a], C. Cecchi[a,b], D. Ciangottini[a,b], L. Fanò[a,b], P. Lariccia[a,b], R. Leonardi[a,b], E. Manoni[a,b], G. Mantovani[a,b], V. Mariani[a,b], M. Menichelli[a], A. Rossi[a,b], A. Santocchia[a,b], D. Spiga[a]

INFN Sezione di Pisa[a], Università di Pisa[b], Scuola Normale Superiore di Pisa[c], Pisa, Italy

K. Androsov[a], P. Azzurri[a,15], G. Bagliesi[a], T. Boccali[a], L. Borrello, R. Castaldi[a], M. A. Ciocci[a,b], R. Dell'Orso[a], G. Fedi[a], L. Giannini[a,c], A. Giassi[a], M. T. Grippo[a,29], F. Ligabue[a,c], T. Lomtadze[a], E. Manca[a,c], G. Mandorli[a,c], L. Martini[a,b], A. Messineo[a,b], F. Palla[a], A. Rizzi[a,b], A. Savoy-Navarro[a,31], P. Spagnolo[a], R. Tenchini[a], G. Tonelli[a,b], A. Venturi[a], P. G. Verdini[a]

INFN Sezione di Roma[a], Sapienza Università di Roma[b], Rome, Italy

L. Barone[a,b], F. Cavallari[a], M. Cipriani[a,b], D. Del Re[a,b,15], E. Di Marco[a,b], M. Diemoz[a], S. Gelli[a,b], E. Longo[a,b], F. Margaroli[a,b], B. Marzocchi[a,b], P. Meridiani[a], G. Organtini[a,b], R. Paramatti[a,b], F. Preiato[a,b], S. Rahatlou[a,b], C. Rovelli[a], F. Santanastasio[a,b]

INFN Sezione di Torino[a], Università di Torino[b], Turin, Italy, Università del Piemonte Orientale[c], Novara, Italy

N. Amapane[a,b], R. Arcidiacono[a,c], S. Argiro[a,b], M. Arneodo[a,c], N. Bartosik[a], R. Bellan[a,b], C. Biino[a], N. Cartiglia[a], M. Costa[a,b], R. Covarelli[a,b], A. Degano[a,b], N. Demaria[a], B. Kiani[a,b], C. Mariotti[a], S. Maselli[a], G. Mazza[a], E. Migliore[a,b], V. Monaco[a,b], E. Monteil[a,b], M. Monteno[a], M. M. Obertino[a,b], L. Pacher[a,b], N. Pastrone[a], M. Pelliccioni[a], G. L. Pinna Angioni[a,b], F. Ravera[a,b], A. Romero[a,b], M. Ruspa[a,c], R. Sacchi[a,b], K. Shchelina[a,b], V. Sola[a], A. Solano[a,b], A. Staiano[a], P. Traczyk[a,b]

INFN Sezione di Trieste[a], Università di Trieste[b], Trieste, Italy

S. Belforte[a], M. Casarsa[a], F. Cossutti[a], G. Della Ricca[a,b], A. Zanetti[a]

Kyungpook National University, Daegu, Korea

D. H. Kim, G. N. Kim, M. S. Kim, J. Lee, S. Lee, S. W. Lee, C. S. Moon, Y. D. Oh, S. Sekmen, D. C. Son, Y. C. Yang

Chonbuk National University, Jeonju, Korea

A. Lee

Chonnam National University, Institute for Universe and Elementary Particles, Kwangju, Korea

H. Kim, D. H. Moon, G. Oh

Hanyang University, Seoul, Korea

J. A. Brochero Cifuentes, J. Goh, T. J. Kim

Korea University, Seoul, Korea

S. Cho, S. Choi, Y. Go, D. Gyun, S. Ha, B. Hong, Y. Jo, Y. Kim, K. Lee, K. S. Lee, S. Lee, J. Lim, S. K. Park, Y. Roh

Seoul National University, Seoul, Korea

J. Almond, J. Kim, J. S. Kim, H. Lee, K. Lee, K. Nam, S. B. Oh, B. C. Radburn-Smith, S. h. Seo, U. K. Yang, H. D. Yoo, G. B. Yu

University of Seoul, Seoul, Korea

M. Choi, H. Kim, J. H. Kim, J. S. H. Lee, I. C. Park

Sungkyunkwan University, Suwon, Korea

Y. Choi, C. Hwang, J. Lee, I. Yu

Vilnius University, Vilnius, Lithuania

V. Dudenas, A. Juodagalvis, J. Vaitkus

National Centre for Particle Physics, Universiti Malaya, Kuala Lumpur, Malaysia

I. Ahmed, Z. A. Ibrahim, M. A. B. Md Ali[32], F. Mohamad Idris[33], W. A. T. Wan Abdullah, M. N. Yusli, Z. Zolkapli

Centro de Investigacion y de Estudios Avanzados del IPN, Mexico City, Mexico

H. Castilla-Valdez, E. De La Cruz-Burelo, M. C. Duran-Osuna, I. Heredia-De La Cruz[34], R. Lopez-Fernandez, J. Mejia Guisao, R. I. Rabadan-Trejo, G. Ramirez-Sanchez, R. Reyes-Almanza, A. Sanchez-Hernandez

Universidad Iberoamericana, Mexico City, Mexico

S. Carrillo Moreno, C. Oropeza Barrera, F. Vazquez Valencia

Benemerita Universidad Autonoma de Puebla, Puebla, Mexico

I. Pedraza, H. A. Salazar Ibarguen, C. Uribe Estrada

Universidad Autónoma de San Luis Potosí, San Luis Potosí, Mexico

A. Morelos Pineda

University of Auckland, Auckland, New Zealand

D. Krofcheck

University of Canterbury, Christchurch, New Zealand

P. H. Butler

National Centre for Physics, Quaid-I-Azam University, Islamabad, Pakistan

A. Ahmad, M. Ahmad, Q. Hassan, H. R. Hoorani, A. Saddique, M. A. Shah, M. Shoaib, M. Waqas

National Centre for Nuclear Research, Swierk, Poland

H. Bialkowska, M. Bluj, B. Boimska, T. Frueboes, M. Górski, M. Kazana, K. Nawrocki, M. Szleper, P. Zalewski

Institute of Experimental Physics, Faculty of Physics, University of Warsaw, Warsaw, Poland

K. Bunkowski, A. Byszuk[35], K. Doroba, A. Kalinowski, M. Konecki, J. Krolikowski, M. Misiura, M. Olszewski, A. Pyskir, M. Walczak

Laboratório de Instrumentação e Física Experimental de Partículas, Lisbon, Portugal

P. Bargassa, C. Beirão Da Cruz E Silva, A. Di Francesco, P. Faccioli, B. Galinhas, M. Gallinaro, J. Hollar, N. Leonardo, L. Lloret Iglesias, M. V. Nemallapudi, J. Seixas, G. Strong, O. Toldaiev, D. Vadruccio, J. Varela

Joint Institute for Nuclear Research, Dubna, Russia

S. Afanasiev, P. Bunin, M. Gavrilenko, I. Golutvin, I. Gorbunov, A. Kamenev, V. Karjavin, A. Lanev, A. Malakhov, V. Matveev[36,37], V. Palichik, V. Perelygin, S. Shmatov, S. Shulha, N. Skatchkov, V. Smirnov, N. Voytishin, A. Zarubin

Petersburg Nuclear Physics Institute, Gatchina, (St. Petersburg), Russia

Y. Ivanov, V. Kim[38], E. Kuznetsova[39], P. Levchenko, V. Murzin, V. Oreshkin, I. Smirnov, V. Sulimov, L. Uvarov, S. Vavilov, A. Vorobyev

Institute for Nuclear Research, Moscow, Russia

Yu. Andreev, A. Dermenev, S. Gninenko, N. Golubev, A. Karneyeu, M. Kirsanov, N. Krasnikov, A. Pashenkov, D. Tlisov, A. Toropin

Institute for Theoretical and Experimental Physics, Moscow, Russia

V. Epshteyn, V. Gavrilov, N. Lychkovskaya, V. Popov, I. Pozdnyakov, G. Safronov, A. Spiridonov, A. Stepennov, M. Toms, E. Vlasov, A. Zhokin

Moscow Institute of Physics and Technology, Moscow, Russia

T. Aushev, A. Bylinkin[37]

National Research Nuclear University 'Moscow Engineering Physics Institute' (MEPhI), Moscow, Russia

R. Chistov[40], M. Danilov[40], P. Parygin, D. Philippov, S. Polikarpov, E. Tarkovskii

P.N. Lebedev Physical Institute, Moscow, Russia

V. Andreev, M. Azarkin[37], I. Dremin[37], M. Kirakosyan[37], A. Terkulov

Skobeltsyn Institute of Nuclear Physics, Lomonosov Moscow State University, Moscow, Russia

A. Baskakov, A. Belyaev, E. Boos, M. Dubinin[41], L. Dudko, A. Ershov, A. Gribushin, V. Klyukhin, O. Kodolova, I. Lokhtin, I. Miagkov, S. Obraztsov, S. Petrushanko, V. Savrin, A. Snigirev

Novosibirsk State University (NSU), Novosibirsk, Russia

V. Blinov[42], Y. Skovpen[42], D. Shtol[42]

State Research Center of Russian Federation, Institute for High Energy Physics, Protvino, Russia

I. Azhgirey, I. Bayshev, S. Bitioukov, D. Elumakhov, V. Kachanov, A. Kalinin, D. Konstantinov, P. Mandrik, V. Petrov, R. Ryutin, A. Sobol, S. Troshin, N. Tyurin, A. Uzunian, A. Volkov

University of Belgrade, Faculty of Physics and Vinca Institute of Nuclear Sciences, Belgrade, Serbia

P. Adzic[43], P. Cirkovic, D. Devetak, M. Dordevic, J. Milosevic, V. Rekovic

Centro de Investigaciones Energéticas Medioambientales y Tecnológicas (CIEMAT), Madrid, Spain

J. Alcaraz Maestre, A. Álvarez Fernández, M. Barrio Luna, M. Cerrada, N. Colino, B. De La Cruz, A. Delgado Peris, A. Escalante Del Valle, C. Fernandez Bedoya, J. P. Fernández Ramos, J. Flix, M. C. Fouz, P. Garcia-Abia, O. Gonzalez Lopez, S. Goy Lopez, J. M. Hernandez, M. I. Josa, D. Moran, A. Pérez-Calero Yzquierdo, J. Puerta Pelayo, A. Quintario Olmeda, I. Redondo, L. Romero, M. S. Soares

Universidad Autónoma de Madrid, Madrid, Spain

C. Albajar, J. F. de Trocóniz, M. Missiroli

Universidad de Oviedo, Oviedo, Spain
J. Cuevas, C. Erice, J. Fernandez Menendez, I. Gonzalez Caballero, J. R. González Fernández, E. Palencia Cortezon, S. Sanchez Cruz, P. Vischia, J. M. Vizan Garcia

Instituto de Física de Cantabria (IFCA), CSIC-Universidad de Cantabria, Santander, Spain
I. J. Cabrillo, A. Calderon, B. Chazin Quero, E. Curras, J. Duarte Campderros, M. Fernandez, J. Garcia-Ferrero, G. Gomez, A. Lopez Virto, J. Marco, C. Martinez Rivero, P. Martinez Ruiz del Arbol, F. Matorras, J. Piedra Gomez, T. Rodrigo, A. Ruiz-Jimeno, L. Scodellaro, N. Trevisani, I. Vila, R. Vilar Cortabitarte

CERN, European Organization for Nuclear Research, Geneva, Switzerland
D. Abbaneo, B. Akgun, E. Auffray, P. Baillon, A. H. Ball, D. Barney, M. Bianco, P. Bloch, A. Bocci, C. Botta, T. Camporesi, R. Castello, M. Cepeda, G. Cerminara, E. Chapon, Y. Chen, D. d'Enterria, A. Dabrowski, V. Daponte, A. David, M. De Gruttola, A. De Roeck, N. Deelen, M. Dobson, T. du Pree, M. Dünser, N. Dupont, A. Elliott-Peisert, P. Everaerts, F. Fallavollita, G. Franzoni, J. Fulcher, W. Funk, D. Gigi, A. Gilbert, K. Gill, F. Glege, D. Gulhan, P. Harris, J. Hegeman, V. Innocente, A. Jafari, P. Janot, O. Karacheban[18], J. Kieseler, V. Knünz, A. Kornmayer, M. J. Kortelainen, C. Lange, P. Lecoq, C. Lourenço, M. T. Lucchini, L. Malgeri, M. Mannelli, A. Martelli, F. Meijers, J. A. Merlin, S. Mersi, E. Meschi, P. Milenovic[44], F. Moortgat, M. Mulders, H. Neugebauer, J. Ngadiuba, S. Orfanelli, L. Orsini, L. Pape, E. Perez, M. Peruzzi, A. Petrilli, G. Petrucciani, A. Pfeiffer, M. Pierini, D. Rabady, A. Racz, T. Reis, G. Rolandi[45], M. Rovere, H. Sakulin, C. Schäfer, C. Schwick, M. Seidel, M. Selvaggi, A. Sharma, P. Silva, P. Sphicas[46], A. Stakia, J. Steggemann, M. Stoye, M. Tosi, D. Treille, A. Triossi, A. Tsirou, V. Veckalns[47], M. Verweij, W. D. Zeuner

Paul Scherrer Institut, Villigen, Switzerland
W. Bertl[†], L. Caminada[48], K. Deiters, W. Erdmann, R. Horisberger, Q. Ingram, H. C. Kaestli, D. Kotlinski, U. Langenegger, T. Rohe, S. A. Wiederkehr

ETH Zurich-Institute for Particle Physics and Astrophysics (IPA), Zurich, Switzerland
M. Backhaus, L. Bäni, P. Berger, L. Bianchini, B. Casal, G. Dissertori, M. Dittmar, M. Donegà, C. Dorfer, C. Grab, C. Heidegger, D. Hits, J. Hoss, G. Kasieczka, T. Klijnsma, W. Lustermann, B. Mangano, M. Marionneau, M. T. Meinhard, D. Meister, F. Micheli, P. Musella, F. Nessi-Tedaldi, F. Pandolfi, J. Pata, F. Pauss, G. Perrin, L. Perrozzi, M. Reichmann, D. A. Sanz Becerra, M. Schönenberger, L. Shchutska, V. R. Tavolaro, K. Theofilatos, M. L. Vesterbacka Olsson, R. Wallny, D. H. Zhu

Universität Zürich, Zurich, Switzerland
T. K. Aarrestad, C. Amsler[49], M. F. Canelli, A. De Cosa, R. Del Burgo, S. Donato, C. Galloni, T. Hreus, B. Kilminster, D. Pinna, G. Rauco, P. Robmann, D. Salerno, K. Schweiger, C. Seitz, Y. Takahashi, A. Zucchetta

National Central University, Chung-Li, Taiwan
V. Candelise, T. H. Doan, Sh. Jain, R. Khurana, C. M. Kuo, W. Lin, A. Pozdnyakov, S. S. Yu

National Taiwan University (NTU), Taipei, Taiwan
Arun Kumar, P. Chang, Y. Chao, K. F. Chen, P. H. Chen, F. Fiori, W.-S. Hou, Y. Hsiung, Y. F. Liu, R.-S. Lu, E. Paganis, A. Psallidas, A. Steen, J. F. Tsai

Chulalongkorn University, Faculty of Science, Department of Physics, Bangkok, Thailand
B. Asavapibhop, K. Kovitanggoon, G. Singh, N. Srimanobhas

Çukurova University, Physics Department, Science and Art Faculty, Adana, Turkey
F. Boran, S. Cerci[50], S. Damarseckin, Z. S. Demiroglu, C. Dozen, I. Dumanoglu, S. Girgis, G. Gokbulut, Y. Guler, I. Hos[51], E. E. Kangal[52], O. Kara, A. Kayis Topaksu, U. Kiminsu, M. Oglakci, G. Onengut[53], K. Ozdemir[54], D. Sunar Cerci[50], B. Tali[50], S. Turkcapar, I. S. Zorbakir, C. Zorbilmez

Middle East Technical University, Physics Department, Ankara, Turkey
B. Bilin, G. Karapinar[55], K. Ocalan[56], M. Yalvac, M. Zeyrek

Bogazici University, Istanbul, Turkey
E. Gülmez, M. Kaya[57], O. Kaya[58], S. Tekten, E. A. Yetkin[59]

Istanbul Technical University, Istanbul, Turkey
M. N. Agaras, S. Atay, A. Cakir, K. Cankocak

Institute for Scintillation Materials of National Academy of Science of Ukraine, Kharkov, Ukraine
B. Grynyov

National Scientific Center, Kharkov Institute of Physics and Technology, Kharkov, Ukraine
L. Levchuk

University of Bristol, Bristol, UK
F. Ball, L. Beck, J. J. Brooke, D. Burns, E. Clement, D. Cussans, O. Davignon, H. Flacher, J. Goldstein, G. P. Heath,
H. F. Heath, J. Jacob, L. Kreczko, D. M. Newbold[60], S. Paramesvaran, T. Sakuma, S. Seif ElNasr-storey, D. Smith,
V. J. Smith

Rutherford Appleton Laboratory, Didcot, UK
K. W. Bell, A. Belyaev[61], C. Brew, R. M. Brown, L. Calligaris, D. Cieri, D. J. A. Cockerill, J. A. Coughlan, K. Harder,
S. Harper, E. Olaiya, D. Petyt, C. H. Shepherd-Themistocleous, A. Thea, I. R. Tomalin, T. Williams

Imperial College, London, UK
G. Auzinger, R. Bainbridge, J. Borg, S. Breeze, O. Buchmuller, A. Bundock, S. Casasso, M. Citron, D. Colling, L. Corpe,
P. Dauncey, G. Davies, A. De Wit, M. Della Negra, R. Di Maria, A. Elwood, Y. Haddad, G. Hall, G. Iles, T. James,
R. Lane, C. Laner, L. Lyons, A.-M. Magnan, S. Malik, L. Mastrolorenzo, T. Matsushita, J. Nash, A. Nikitenko[5],
V. Palladino, M. Pesaresi, D. M. Raymond, A. Richards, A. Rose, E. Scott, C. Seez, A. Shtipliyski, S. Summers, A. Tapper,
K. Uchida, M. Vazquez Acosta[62], T. Virdee[15], N. Wardle, D. Winterbottom, J. Wright, S. C. Zenz

Brunel University, Uxbridge, UK
J. E. Cole, P. R. Hobson, A. Khan, P. Kyberd, I. D. Reid, P. Symonds, L. Teodorescu, M. Turner, S. Zahid

Baylor University, Waco, USA
A. Borzou, K. Call, J. Dittmann, K. Hatakeyama, H. Liu, N. Pastika, C. Smith

Catholic University of America, Washington, DC, USA
R. Bartek, A. Dominguez

The University of Alabama, Tuscaloosa, USA
A. Buccilli, S. I. Cooper, C. Henderson, P. Rumerio, C. West

Boston University, Boston, USA
D. Arcaro, A. Avetisyan, T. Bose, D. Gastler, D. Rankin, C. Richardson, J. Rohlf, L. Sulak, D. Zou

Brown University, Providence, USA
G. Benelli, D. Cutts, A. Garabedian, M. Hadley, J. Hakala, U. Heintz, J. M. Hogan, K. H. M. Kwok, E. Laird,
G. Landsberg, J. Lee, Z. Mao, M. Narain, J. Pazzini, S. Piperov, S. Sagir, R. Syarif, D. Yu

University of California, Davis, Davis, USA
R. Band, C. Brainerd, R. Breedon, D. Burns, M. Calderon De La Barca Sanchez, M. Chertok, J. Conway, R. Conway,
P. T. Cox, R. Erbacher, C. Flores, G. Funk, M. Gardner, W. Ko, R. Lander, C. Mclean, M. Mulhearn, D. Pellett, J. Pilot,
S. Shalhout, M. Shi, J. Smith, D. Stolp, K. Tos, M. Tripathi, Z. Wang

University of California, Los Angeles, USA
M. Bachtis, C. Bravo, R. Cousins, A. Dasgupta, A. Florent, J. Hauser, M. Ignatenko, N. Mccoll, S. Regnard, D. Saltzberg,
C. Schnaible, V. Valuev

University of California, Riverside, Riverside, USA
E. Bouvier, K. Burt, R. Clare, J. Ellison, J. W. Gary, S. M. A. Ghiasi Shirazi, G. Hanson, J. Heilman, E. Kennedy,
F. Lacroix, O. R. Long, M. Olmedo Negrete, M. I. Paneva, W. Si, L. Wang, H. Wei, S. Wimpenny, B. R. Yates

University of California, San Diego, La Jolla, USA
J. G. Branson, S. Cittolin, M. Derdzinski, D. Gilbert, B. Hashemi, A. Holzner, D. Klein, G. Kole, V. Krutelyov, J. Letts,
I. Macneill, M. Masciovecchio, D. Olivito, S. Padhi, M. Pieri, M. Sani, V. Sharma, S. Simon, M. Tadel, A. Vartak,
S. Wasserbaech[63], J. Wood, F. Würthwein, A. Yagil, G. Zevi Della Porta

University of California, Santa Barbara-Department of Physics, Santa Barbara, USA

N. Amin, R. Bhandari, J. Bradmiller-Feld, C. Campagnari, A. Dishaw, V. Dutta, M. Franco Sevilla, C. George, F. Golf, L. Gouskos, J. Gran, R. Heller, J. Incandela, S. D. Mullin, A. Ovcharova, H. Qu, J. Richman, D. Stuart, I. Suarez, J. Yoo

California Institute of Technology, Pasadena, USA

D. Anderson, J. Bendavid, A. Bornheim, J. M. Lawhorn, H. B. Newman, T. Nguyen, C. Pena, M. Spiropulu, J. R. Vlimant, S. Xie, Z. Zhang, R. Y. Zhu

Carnegie Mellon University, Pittsburgh, USA

M. B. Andrews, T. Ferguson, T. Mudholkar, M. Paulini, J. Russ, M. Sun, H. Vogel, I. Vorobiev, M. Weinberg

University of Colorado Boulder, Boulder, USA

J. P. Cumalat, W. T. Ford, F. Jensen, A. Johnson, M. Krohn, S. Leontsinis, T. Mulholland, K. Stenson, S. R. Wagner

Cornell University, Ithaca, USA

J. Alexander, J. Chaves, J. Chu, S. Dittmer, K. Mcdermott, N. Mirman, J. R. Patterson, D. Quach, A. Rinkevicius, A. Ryd, L. Skinnari, L. Soffi, S. M. Tan, Z. Tao, J. Thom, J. Tucker, P. Wittich, M. Zientek

Fermi National Accelerator Laboratory, Batavia, USA

S. Abdullin, M. Albrow, M. Alyari, G. Apollinari, A. Apresyan, A. Apyan, S. Banerjee, L. A. T. Bauerdick, A. Beretvas, J. Berryhill, P. C. Bhat, G. Bolla[†], K. Burkett, J. N. Butler, A. Canepa, G. B. Cerati, H. W. K. Cheung, F. Chlebana, M. Cremonesi, J. Duarte, V. D. Elvira, J. Freeman, Z. Gecse, E. Gottschalk, L. Gray, D. Green, S. Grünendahl, O. Gutsche, R. M. Harris, S. Hasegawa, J. Hirschauer, Z. Hu, B. Jayatilaka, S. Jindariani, M. Johnson, U. Joshi, B. Klima, B. Kreis, S. Lammel, D. Lincoln, R. Lipton, M. Liu, T. Liu, R. Lopes De Sá, J. Lykken, K. Maeshima, N. Magini, J. M. Marraffino, D. Mason, P. McBride, P. Merkel, S. Mrenna, S. Nahn, V. O'Dell, K. Pedro, O. Prokofyev, G. Rakness, L. Ristori, B. Schneider, E. Sexton-Kennedy, A. Soha, W. J. Spalding, L. Spiegel, S. Stoynev, J. Strait, N. Strobbe, L. Taylor, S. Tkaczyk, N. V. Tran, L. Uplegger, E. W. Vaandering, C. Vernieri, M. Verzocchi, R. Vidal, M. Wang, H. A. Weber, A. Whitbeck

University of Florida, Gainesville, USA

D. Acosta, P. Avery, P. Bortignon, D. Bourilkov, A. Brinkerhoff, A. Carnes, M. Carver, D. Curry, R. D. Field, I. K. Furic, J. Konigsberg, A. Korytov, K. Kotov, P. Ma, K. Matchev, H. Mei, G. Mitselmakher, D. Rank, D. Sperka, N. Terentyev, L. Thomas, J. Wang, S. Wang, J. Yelton

Florida International University, Miami, USA

Y. R. Joshi, S. Linn, P. Markowitz, J. L. Rodriguez

Florida State University, Tallahassee, USA

A. Ackert, T. Adams, A. Askew, S. Hagopian, V. Hagopian, K. F. Johnson, T. Kolberg, G. Martinez, T. Perry, H. Prosper, A. Saha, A. Santra, V. Sharma, R. Yohay

Florida Institute of Technology, Melbourne, USA

M. M. Baarmand, V. Bhopatkar, S. Colafranceschi, M. Hohlmann, D. Noonan, T. Roy, F. Yumiceva

University of Illinois at Chicago (UIC), Chicago, USA

M. R. Adams, L. Apanasevich, D. Berry, R. R. Betts, R. Cavanaugh, X. Chen, O. Evdokimov, C. E. Gerber, D. A. Hangal, D. J. Hofman, K. Jung, J. Kamin, I. D. Sandoval Gonzalez, M. B. Tonjes, H. Trauger, N. Varelas, H. Wang, Z. Wu, J. Zhang

The University of Iowa, Iowa City, USA

B. Bilki[64], W. Clarida, K. Dilsiz[65], S. Durgut, R. P. Gandrajula, M. Haytmyradov, V. Khristenko, J.-P. Merlo, H. Mermerkaya[66], A. Mestvirishvili, A. Moeller, J. Nachtman, H. Ogul[67], Y. Onel, F. Ozok[68], A. Penzo, C. Snyder, E. Tiras, J. Wetzel, K. Yi

Johns Hopkins University, Baltimore, USA

B. Blumenfeld, A. Cocoros, N. Eminizer, D. Fehling, L. Feng, A. V. Gritsan, P. Maksimovic, J. Roskes, U. Sarica, M. Swartz, M. Xiao, C. You

The University of Kansas, Lawrence, USA

A. Al-bataineh, P. Baringer, A. Bean, S. Boren, J. Bowen, J. Castle, S. Khalil, A. Kropivnitskaya, D. Majumder, W. Mcbrayer, M. Murray, C. Royon, S. Sanders, E. Schmitz, J. D. Tapia Takaki, Q. Wang

Kansas State University, Manhattan, USA

A. Ivanov, K. Kaadze, Y. Maravin, A. Mohammadi, L. K. Saini, N. Skhirtladze, S. Toda

Lawrence Livermore National Laboratory, Livermore, USA

F. Rebassoo, D. Wright

University of Maryland, College Park, USA

C. Anelli, A. Baden, O. Baron, A. Belloni, B. Calvert, S. C. Eno, Y. Feng, C. Ferraioli, N. J. Hadley, S. Jabeen, G. Y. Jeng, R. G. Kellogg, J. Kunkle, A. C. Mignerey, F. Ricci-Tam, Y. H. Shin, A. Skuja, S. C. Tonwar

Massachusetts Institute of Technology, Cambridge, USA

D. Abercrombie, B. Allen, V. Azzolini, R. Barbieri, A. Baty, R. Bi, S. Brandt, W. Busza, I. A. Cali, M. D'Alfonso, Z. Demiragli, G. Gomez Ceballos, M. Goncharov, D. Hsu, M. Hu, Y. Iiyama, G. M. Innocenti, M. Klute, D. Kovalskyi, Y. S. Lai, Y.-J. Lee, A. Levin, P. D. Luckey, B. Maier, A. C. Marini, C. Mcginn, C. Mironov, S. Narayanan, X. Niu, C. Paus, C. Roland, G. Roland, J. Salfeld-Nebgen, G. S. F. Stephans, K. Tatar, D. Velicanu, J. Wang, T. W. Wang, B. Wyslouch

University of Minnesota, Minneapolis, USA

A. C. Benvenuti, R. M. Chatterjee, A. Evans, P. Hansen, J. Hiltbrand, S. Kalafut, Y. Kubota, Z. Lesko, J. Mans, S. Nourbakhsh, N. Ruckstuhl, R. Rusack, J. Turkewitz, M. A. Wadud

University of Mississippi, Oxford, USA

J. G. Acosta, S. Oliveros

University of Nebraska-Lincoln, Lincoln, USA

E. Avdeeva, K. Bloom, D. R. Claes, C. Fangmeier, R. Gonzalez Suarez, R. Kamalieddin, I. Kravchenko, J. Monroy, J. E. Siado, G. R. Snow, B. Stieger

State University of New York at Buffalo, Buffalo, USA

J. Dolen, A. Godshalk, C. Harrington, I. Iashvili, D. Nguyen, A. Parker, S. Rappoccio, B. Roozbahani

Northeastern University, Boston, USA

G. Alverson, E. Barberis, A. Hortiangtham, A. Massironi, D. M. Morse, T. Orimoto, R. Teixeira De Lima, D. Trocino, D. Wood

Northwestern University, Evanston, USA

S. Bhattacharya, O. Charaf, K. A. Hahn, N. Mucia, N. Odell, B. Pollack, M. H. Schmitt, K. Sung, M. Trovato, M. Velasco

University of Notre Dame, Notre Dame, USA

N. Dev, M. Hildreth, K. Hurtado Anampa, C. Jessop, D. J. Karmgard, N. Kellams, K. Lannon, N. Loukas, N. Marinelli, F. Meng, C. Mueller, Y. Musienko[36], M. Planer, A. Reinsvold, R. Ruchti, G. Smith, S. Taroni, M. Wayne, M. Wolf, A. Woodard

The Ohio State University, Columbus, USA

J. Alimena, L. Antonelli, B. Bylsma, L. S. Durkin, S. Flowers, B. Francis, A. Hart, C. Hill, W. Ji, B. Liu, W. Luo, D. Puigh, B. L. Winer, H. W. Wulsin

Princeton University, Princeton, USA

S. Cooperstein, O. Driga, P. Elmer, J. Hardenbrook, P. Hebda, S. Higginbotham, D. Lange, J. Luo, D. Marlow, K. Mei, I. Ojalvo, J. Olsen, C. Palmer, P. Piroué, D. Stickland, C. Tully

University of Puerto Rico, Mayaguez, USA

S. Malik, S. Norberg

Purdue University, West Lafayette, USA

A. Barker, V. E. Barnes, S. Das, S. Folgueras, L. Gutay, M. K. Jha, M. Jones, A. W. Jung, A. Khatiwada, D. H. Miller, N. Neumeister, C. C. Peng, H. Qiu, J. F. Schulte, J. Sun, F. Wang, W. Xie

Purdue University Northwest, Hammond, USA

T. Cheng, N. Parashar, J. Stupak

Rice University, Houston, USA

A. Adair, Z. Chen, K. M. Ecklund, S. Freed, F. J. M. Geurts, M. Guilbaud, M. Kilpatrick, W. Li, B. Michlin, M. Northup, B. P. Padley, J. Roberts, J. Rorie, W. Shi, Z. Tu, J. Zabel, A. Zhang

University of Rochester, Rochester, USA

A. Bodek, P. de Barbaro, R. Demina, Y. T. Duh, T. Ferbel, M. Galanti, A. Garcia-Bellido, J. Han, O. Hindrichs, A. Khukhunaishvili, K. H. Lo, P. Tan, M. Verzetti

The Rockefeller University, New York, USA

R. Ciesielski, K. Goulianos, C. Mesropian

Rutgers, The State University of New Jersey, Piscataway, USA

A. Agapitos, J. P. Chou, Y. Gershtein, T. A. Gómez Espinosa, E. Halkiadakis, M. Heindl, E. Hughes, S. Kaplan, R. Kunnawalkam Elayavalli, S. Kyriacou, A. Lath, R. Montalvo, K. Nash, M. Osherson, H. Saka, S. Salur, S. Schnetzer, D. Sheffield, S. Somalwar, R. Stone, S. Thomas, P. Thomassen, M. Walker

University of Tennessee, Knoxville, USA

A. G. Delannoy, M. Foerster, J. Heideman, G. Riley, K. Rose, S. Spanier, K. Thapa

Texas A & M University, College Station, USA

O. Bouhali[69], A. Castaneda Hernandez[69], A. Celik, M. Dalchenko, M. De Mattia, A. Delgado, S. Dildick, R. Eusebi, J. Gilmore, T. Huang, T. Kamon[70], R. Mueller, Y. Pakhotin, R. Patel, A. Perloff, L. Perniè, D. Rathjens, A. Safonov, A. Tatarinov, K. A. Ulmer

Texas Tech University, Lubbock, USA

N. Akchurin, J. Damgov, F. De Guio, P. R. Dudero, J. Faulkner, E. Gurpinar, S. Kunori, K. Lamichhane, S. W. Lee, T. Libeiro, T. Peltola, S. Undleeb, I. Volobouev, Z. Wang

Vanderbilt University, Nashville, USA

S. Greene, A. Gurrola, R. Janjam, W. Johns, C. Maguire, A. Melo, H. Ni, K. Padeken, P. Sheldon, S. Tuo, J. Velkovska, Q. Xu

University of Virginia, Charlottesville, USA

M. W. Arenton, P. Barria, B. Cox, R. Hirosky, M. Joyce, A. Ledovskoy, H. Li, C. Neu, T. Sinthuprasith, Y. Wang, E. Wolfe, F. Xia

Wayne State University, Detroit, USA

R. Harr, P. E. Karchin, N. Poudyal, J. Sturdy, P. Thapa, S. Zaleski

University of Wisconsin-Madison, Madison, WI, USA

M. Brodski, J. Buchanan, C. Caillol, S. Dasu, L. Dodd, S. Duric, B. Gomber, M. Grothe, M. Herndon, A. Hervé, U. Hussain, P. Klabbers, A. Lanaro, A. Levine, K. Long, R. Loveless, G. Polese, T. Ruggles, A. Savin, N. Smith, W. H. Smith, D. Taylor, N. Woods

† **Deceased**

1: Also at Vienna University of Technology, Vienna, Austria
2: Also at State Key Laboratory of Nuclear Physics and Technology, Peking University, Beijing, China
3: Also at Universidade Estadual de Campinas, Campinas, Brazil
4: Also at Universidade Federal de Pelotas, Pelotas, Brazil
5: Also at Université Libre de Bruxelles, Brussels, Belgium
6: Also at Institute for Theoretical and Experimental Physics, Moscow, Russia
7: Also at Joint Institute for Nuclear Research, Dubna, Russia
8: Also at Suez University, Suez, Egypt
9: Now at British University in Egypt, Cairo, Egypt

10: Now at Helwan University, Cairo, Egypt

11: Also at Université de Haute Alsace, Mulhouse, France

12: Also at Skobeltsyn Institute of Nuclear Physics, Lomonosov Moscow State University, Moscow, Russia

13: Also at Tbilisi State University, Tbilisi, Georgia

14: Also at Ilia State University, Tbilisi, Georgia

15: Also at CERN, European Organization for Nuclear Research, Geneva, Switzerland

16: Also at RWTH Aachen University, III. Physikalisches Institut A, Aachen, Germany

17: Also at University of Hamburg, Hamburg, Germany

18: Also at Brandenburg University of Technology, Cottbus, Germany

19: Also at MTA-ELTE Lendület CMS Particle and Nuclear Physics Group, Eötvös Loránd University, Budapest, Hungary

20: Also at Institute of Nuclear Research ATOMKI, Debrecen, Hungary

21: Also at Institute of Physics, University of Debrecen, Debrecen, Hungary

22: Also at Indian Institute of Technology Bhubaneswar, Bhubaneswar, India

23: Also at Institute of Physics, Bhubaneswar, India

24: Also at University of Visva-Bharati, Santiniketan, India

25: Also at University of Ruhuna, Matara, Sri Lanka

26: Also at Isfahan University of Technology, Isfahan, Iran

27: Also at Yazd University, Yazd, Iran

28: Also at Plasma Physics Research Center, Science and Research Branch, Islamic Azad University, Tehran, Iran

29: Also at Università degli Studi di Siena, Siena, Italy

30: Also at INFN Sezione di Milano-Bicocca; Università di Milano-Bicocca, Milano, Italy

31: Also at Purdue University, West Lafayette, USA

32: Also at International Islamic University of Malaysia, Kuala Lumpur, Malaysia

33: Also at Malaysian Nuclear Agency, MOSTI, Kajang, Malaysia

34: Also at Consejo Nacional de Ciencia y Tecnología, Mexico City, Mexico

35: Also at Warsaw University of Technology, Institute of Electronic Systems, Warsaw, Poland

36: Also at Institute for Nuclear Research, Moscow, Russia

37: Now at National Research Nuclear University 'Moscow Engineering Physics Institute' (MEPhI), Moscow, Russia

38: Also at St. Petersburg State Polytechnical University, St. Petersburg, Russia

39: Also at University of Florida, Gainesville, USA

40: Also at P.N. Lebedev Physical Institute, Moscow, Russia

41: Also at California Institute of Technology, Pasadena, USA

42: Also at Budker Institute of Nuclear Physics, Novosibirsk, Russia

43: Also at Faculty of Physics, University of Belgrade, Belgrade, Serbia

44: Also at University of Belgrade, Faculty of Physics and Vinca Institute of Nuclear Sciences, Belgrade, Serbia

45: Also at Scuola Normale e Sezione dell'INFN, Pisa, Italy

46: Also at National and Kapodistrian University of Athens, Athens, Greece

47: Also at Riga Technical University, Riga, Latvia

48: Also at Universität Zürich, Zurich, Switzerland

49: Also at Stefan Meyer Institute for Subatomic Physics (SMI), Vienna, Austria

50: Also at Adiyaman University, Adiyaman, Turkey

51: Also at Istanbul Aydin University, Istanbul, Turkey

52: Also at Mersin University, Mersin, Turkey

53: Also at Cag University, Mersin, Turkey

54: Also at Piri Reis University, Istanbul, Turkey

55: Also at Izmir Institute of Technology, Izmir, Turkey

56: Also at Necmettin Erbakan University, Konya, Turkey

57: Also at Marmara University, Istanbul, Turkey

58: Also at Kafkas University, Kars, Turkey

59: Also at Istanbul Bilgi University, Istanbul, Turkey

60: Also at Rutherford Appleton Laboratory, Didcot, UK

61: Also at School of Physics and Astronomy, University of Southampton, Southampton, UK

62: Also at Instituto de Astrofísica de Canarias, La Laguna, Spain

63: Also at Utah Valley University, Orem, USA
64: Also at Beykent University, Istanbul, Turkey
65: Also at Bingol University, Bingöl, Turkey
66: Also at Erzincan University, Erzincan, Turkey
67: Also at Sinop University, Sinop, Turkey
68: Also at Mimar Sinan University, Istanbul, Istanbul, Turkey
69: Also at Texas A&M University at Qatar, Doha, Qatar
70: Also at Kyungpook National University, Daegu, Korea